

AN ABSTRACT OF THE THESIS OF

Priyanka Singla for the degree of Master of Science in Microbiology presented on March 5, 2021.

Title: Investigating the Impact of Gut Microbiota on Rodent Behavior and their Interaction with Enteroendocrine Cells.

Abstract approved: \_\_\_\_\_

Maude M. David

Gut-brain communication consists of bidirectional routes between cognitive centers of the brain and peripheral intestines. This bidirectional communication is the result of the interplay between enteroendocrine cells (EECs), enteric nervous system, central nervous system, the vagus nerve, and our microbiota. Multiple studies have associated gut microbial dysbiosis with neurological disorders or altered behavioral phenotype. Specifically, recent work in Autism Spectrum Disorder associates *Clostridium* species in the etiology of the disorder, as well as other neuro-developmental disorders. In order to define the potential role of the *Clostridium* bacteria in the etiology of ASD, we focused on *Clostridium celatum*, a bacteria found to be enriched in children with ASD and part of normal human gut flora and is non-pathogenic. We studied the impact of *C. celatum* on the core symptoms of autism in a rodent model by feeding *C. celatum* to C57BL/6 mice and Maternal Immune Activation (MIA) mice model of autism, and by performing various behavioral tests related to anxiety and sociability, we observed that we were able to modulate behavioral phenotypes in mice using *C. celatum*.

The microbiota is thought to interact with the brain through a number of pathways including the immune system, microbial metabolites, enteroendocrine cells (EECs), and the vagus nerve. The focus of the second part of the project was to determine if *C. celatum* and the other taxa in the gut microbiota can directly interact with these gut sensory cells and eventually transduce the signals to the brain via the vagus nerve. To do so, we successfully isolated and

cultured EECs from the small intestine of CCK-GFP transgenic mice and crosslinked them with all the gut microbiota using a cell impermeable cross-linking reagent. 16S rRNA sequencing analysis of samples with *C. celatum* indicated that *C. celatum* doesn't cross-link with EECs. However, analysis of the samples containing all the gut microbiota crosslinked with EECs suggested a significantly higher abundance of the taxa belonging to the *Rhizobiaceae* and *Lactobacillaceae* families that cross-linked with EECs.

©Copyright by Priyanka Singla  
March 5, 2021  
All Rights Reserved

Investigating the Impact of the Gut Microbiota on Rodent Behavior and their Interaction with  
Enteroendocrine Cells

by  
Priyanka Singla

A THESIS

submitted to

Oregon State University

in partial fulfillment of  
the requirements for the  
degree of

Master of Science

Presented March 5, 2021  
Commencement June 2021

Master of Science thesis of Priyanka Singla presented on March 5, 2021

APPROVED:

---

Major Professor, representing Microbiology

---

Head of the Department of Microbiology

---

Dean of the Graduate School

I understand that my thesis will become part of the permanent collection of Oregon State University libraries. My signature below authorizes release of my thesis to any reader upon request.

---

Priyanka Singla, Author

## ACKNOWLEDGEMENTS

I would firstly like to thank my advisor, Dr. Maude M. David, for all of her help and constant support and guidance in completing this project. I must also thank our collaborators, Prof. Rodger Liddle, from Duke University for providing us with the mice colony for this project, and Prof. Kathy Magnusson for helping us with the nodose ganglion dissection. Also thanks to my other committee members Dr. Mahfuz Sarkar, Dr. Brianna Beechler for their invaluable feedback.

I am also incredibly grateful to Dr. Melanie Maya Kaelberer and Bohorquez lab from Duke University for providing us with the protocol for this project. Further, I would like to express my sincere gratitude to Dr. Maria Franco and Dr. Alvaro Estevez for their insightful suggestions and unparalleled support throughout this project. I especially want to thank everyone in the David Lab for their input and continuous support. I would particularly like to thank Annabel Martin-Varnum, the undergraduate researcher in our lab, for her assistance throughout this project. I would also like to thank Mark Dasenko in OSU Center for Genome Research and Biocomputing for sequencing.

Finally, I would like to thank all my friends and family back in India and in the U.S for their love and infinite support.

## TABLE OF CONTENTS

	<u>Page</u>
1. Introduction.....	1
2. Literature Review.....	3
2.1 <i>Clostridium celatum</i> in the Gut-Brain Axis.....	3
2.1.1 The gut microbiome.....	3
2.1.2 <i>Clostridium celatum</i> in the human gut.....	3
2.1.3 The gut microbiota-brain axis.....	4
2.2 Enteroendocrine cells (EECs), vagal nerve, and the gut microbiome.....	5
2.2.1 Enteroendocrine cells in the gut.....	5
2.2.2 Different types of EECs.....	5
2.2.3 Chemosensation by EECs.....	7
2.2.4 Neuropods discovered in EECs.....	7
2.2.5 EECs connection with neurons via neuropods.....	8
2.2.6 Neural circuit between EECs and the brain via vagus nerve.....	9
2.2.7 Interactions between gut microbiome and EECs.....	10
3. Materials and Methods.....	12
3.1 Comparative and phylogenetic analysis of <i>C. celatum</i> genome.....	12
3.2 Growing <i>Clostridium celatum</i> in anaerobic chamber.....	13
3.3 Animals.....	13
3.3.1 C57BL/6 mice.....	13
3.3.2 CCK-GFP mice colony establishment and management.....	14
3.4 Viability of <i>C. celatum</i> in apple juice.....	15
3.5 Behavior tests.....	15
3.5.1 Open Field Habituation test.....	15

## TABLE OF CONTENTS (Continued)

	<u>Page</u>
3.5.2 Elevated Plus Maze.....	15
3.5.3 Marble Burying.....	16
3.5.4 Three Chambered Sociability and Social Novelty Test.....	16
3.6 Genotyping of CCK-GFP mice.....	16
3.6.1 DNA extraction.....	16
3.6.2 PCR setup.....	17
3.6.3 Product Analysis.....	17
3.7 Magnetic sorting of EECs.....	18
3.8 EECs culturing.....	18
3.9 Neurons culturing from nodose ganglion.....	19
3.10 EECs and neurons co-culturing.....	19
3.11 EECs cross-linking with gut microbiota.....	20
3.11.1 EECs culturing and storage of gut contents.....	20
3.11.2 Bacterial labeling and cross-linking with EECs.....	20
3.11.3 DNA extraction from the cross-linked cells.....	20
3.11.4 16S rRNA amplification and sequencing.....	20
4. Results.....	22
4.1 <i>Clostridium celatum</i> in the gut-brain axis.....	22
4.1.1 Comparative genomic and phylogenetic analysis of <i>C. celatum</i> .....	22
4.1.2 Viability of <i>C. celatum</i> in apple juice.....	24
4.1.3 Open Field Habituation test.....	26
4.1.4 Elevated Plus Maze.....	28
4.1.5 Marble Burying.....	31

## TABLE OF CONTENTS (Continued)

	<u>Page</u>
4.1.6 Three Chambered Sociability and Social Novelty test.....	32
4.2 Enteroendocrine cells (EEC), vagal nerve and the gut microbiome.....	36
4.2.1 EECs viability after dissociation.....	36
4.2.2 Magnetic sorting of EECs.....	37
4.2.3 EECs sorted by FACS and cultured overnight.....	39
4.2.4 EECs-neurons co-culturing.....	39
4.2.5 EECs-gut microbiota crosslinking.....	40
4.2.6 EECs- <i>C. celatum</i> crosslinking.....	47
5. Discussion.....	48
5.1 <i>C. celatum</i> in the gut- brain axis.....	48
5.2 Enteroendocrine cells, vagal nerve, and the gut microbiome.....	50
5.2.1 Optimization of isolation of EECs.....	50
5.2.2 Crosslinking of gut microbiota with EECs.....	51
6. Conclusion.....	53
Bibliography.....	54

## LIST OF FIGURES

<u>Figures</u>	<u>Page</u>
1. Open and closed type of EECs .....	5
2. Different types and location of EECs in the Gastrointestinal Tract.....	6
3. Enteric-glia and EECs connection.....	8
4. Connection of a single CCK-GFP EEC (green) isolated by FACS, with a sensory neuron (Dil-labeled, red), imaged using fluorescence incubator microscope.....	8
5. Enteroendocrine cell communication in the gut.....	10
6. Four different types of treatment groups for mice for the study.....	14
7. Constrained Principal Coordinate analysis (PCoA) plot of Bray–Curtis distances between selected KEGG Orthologs of <i>Clostridium celatum</i> and closely related <i>Clostridium</i> .....	23
8. Phylogenetic tree of 248 <i>Clostridium</i> genomes based on full length 16S rRNA.....	24
9. Viability of <i>C. celatum</i> culture in apple juice over a period of 48 hours .....	25
10. Time per entry in seconds in the center arena of the open field during the 3 days of habituation.....	27
11. Total distance traveled in the open field during the 3 days of habituation.....	28
12. Time in seconds spent in the closed arms of the elevated plus maze.....	29
13. Time in seconds spent in the open arms of the elevated plus maze.....	30
14. Ratio of time spent in open arms to total time spent in closed and open arms of the elevated plus maze.....	30
15. Number of marbles buried by the four treatment groups of mice.....	31
16. Time spent in seconds with empty cup (novel object) and stranger 1(mouse) for all the treatment in the stage 2 of the test.....	33
17. Time spent in seconds with Stranger 1 (mouse) across all the treatments in the stage 2 of the test.....	34
18. Time spent in seconds with stranger 1 and stranger 2 during the final stage of the test, compared for all the treatment groups of mice.....	35
19. Time spent in seconds with stranger 2 in the final stage of the test.....	36

## LIST OF FIGURES (Continued)

<u>Figures</u>	<u>Page</u>
20. Gut epithelial cells after dissociation, stained with trypan blue, to measure cell viability by loading the hemocytometer.....	37
21. Unlabeled cells that passed through the column.....	38
22. Labeled cells retained in the column and collected by flushing the column with a separation buffer.....	38
23. Flow cytometry analysis of the gut epithelial cells labeled with PE-conjugated Anti-Cld-4 antibody.....	39
24. Entero-endocrine cells visualised under epifluorescent microscope after an overnight incubation.....	39
25. Co-culture of vagal nodose neurons and EECs.....	40
26. Principal Coordinate analysis (PCoA) plot of Bray- Curtis distances between all EEC-Bacterial Wash and EEC-cross linked samples.....	40
27. Comparable sequencing depth of EEC- BW and EEC-cross linked samples.....	41
28. Relative abundance of taxa found in top 50 most abundant ASVs in EEC- BW and EEC-cross linked samples at the genus level.....	41
29. FDR corrected Wilcox test. Abundance plot of significant different ASVs (annotated at Family level) in EEC- BW and EEC- Cross-link Amendment.....	42
30. Phylogenetic tree of family <i>Rhizobiaceae</i> showing significant different ASVs.....	43
31. ANCOM test. Abundance plot of significant different ASVs (annotated at Family level) in EEC- BW and EEC- Cross-link Amendment.....	44
32. Phylogenetic tree of family <i>Rhizobiaceae</i> showing significant different ASVs (ANCOM test) in EEC-Xlink amendment.....	45
33. Abundance plot of significant different ASVs (annotated at Family level) in Neg- BW and Neg- Cross-link Amendment.....	45
34. Phylogenetic tree of family <i>Lactobacillaceae</i> showing significant different ASVs.....	46
35. Abundance of ASVs similar to <i>C. celatum</i> (>90% similarity).....	47

## LIST OF TABLES

<u>Tables</u>	<u>Page</u>
1. Pathogenicity designations used for the comparative analysis of <i>C. celatum</i> genome.....	12
2. PCR master mix components for CCK-GFP mice genotyping.....	17
3. 16S PCR master mix components.....	21
4. Different types of amendments/samples used in crosslinking data analysis.....	21
5. CFU/ml of <i>C. celatum</i> in apple juice at various time intervals.....	25
6. Significant ASVs in EEC-BW and EEC-cross-link samples, classified at the phylum, order, family and genus level.....	44

## 1. Introduction

The gut-brain axis refers to the bidirectional communication that takes place between the central nervous system (CNS) and gastrointestinal (GI) tract. While recent studies have now established associations between the gut microbiota and the brain function (Mohajeri et al., 2018)(Cryan & Dinan, 2012), there is a lack of knowledge in identifying specific mechanisms by which the gut microbiota and central nervous system interact. Several molecular mechanisms have been hypothesized to be involved in this interaction, for instance, the microbially derived molecules can alter the brain and behavior by acting on the mucosal immune system (Salvo-Romero et al., 2020). It has also been shown that they may cross the intestinal barrier and enter systemic circulation (Parker et al., 2020). Besides, these molecules can propagate signals by acting locally through interaction with enteroendocrine cells (EECs) in the gut which can activate closely located afferent vagal nerve terminals that send signals to the brain (Martin et al., 2018). In this document, we will study the interactions between gut microbiota and the brain and we will focus on the local mechanism of action via EECs and vagus nerve.

In the first part of the project, we study the impact of gut microbiota on behavioral phenotypes. While the beneficial effects of gut microbiome on behavior have been well established, *Bifidobacterium longum* and *Lactobacillus helveticus*, for example, alleviated psychological distress in volunteer subjects (Messaoudi et al., 2011), very few studies have considered the negative impacts of gut microbiota on behavior. **Our central hypothesis is that alterations in the gut microbiota using single strain of bacteria can negatively modulate the behavioral outcomes in mice.** Here, we focus on *Clostridium celatum*, because it is a non-pathogenic bacteria (BSL-1), part of normal gut flora of humans and mice and was found to be enriched in children with Autism in a crowdsourced study (David et al., n.d.). Significantly elevated levels of *Clostridium* species have also been reported in other autism related studies (Angelis et al., 2013; Finegold et al., 2002). We feed the mice with *C. celatum* and perform several behavioral assays related to anxiety and sociability.

**In the second part of the project, we hypothesize that the gut microbiota can potentially send signals to the brain via direct interactions with EECs and vagus nerve.**

Many studies indicate that EECs are key sensors of gut microbiota and/or microbial metabolites and the role of vagus nerve has been well established as a modulator between the brain and the gastrointestinal tract in major psychiatric conditions (Breit et al., 2018). Cardiac vagal tone (CVT) is now considered as a physiological index of stress, considering the role of the vagus nerve in modulating stress (Porges, 1995). In a study, CVT was found to be significantly lower in children with autism compared with healthy controls (Ming et al., 2005). Diminished vagal activity has also been associated with autism spectrum disorder (ASD) and thus Vagal nerve stimulation has been emerging as a potential behavioral therapy for autism (Engineer et al., 2017). For this part of the study, we first optimize the isolation of EECs from other intestinal epithelial cells. We try several methods to isolate them including magnetic sorting and finally by fluorescence activated cell sorting (FACS), we successfully isolate and culture GFP-labeled EECs. Further, by co-culturing EECs and vagal nodose neurons, we optimize recapitulation of the connection between EECs and the vagus nerve. (Kaelberer et al., 2018). Finally, by covalently cross-linking EECs with the gut microbiota, we aim to determine if *C. celatum* or other taxa in the gut microbiota can interact with EECs.

## 2. Literature Review

### 2.1 *Clostridium celatum* in the Gut-Brain Axis

#### 2.1.1 *The gut microbiome*

The human GI tract contains around  $10^{13}$  microorganisms, which consists of more than 1000 species and around 7000 strains (Cryan & Dinan, 2012). The establishment of the gut microbiome depends on many factors like birth process, infant feeding method, diet, exercise, stress, consumption of antibiotics, so it can vary greatly between different individuals (Voreades et al., 2014).

The gut microbiome plays an important role in maintaining gut homeostasis, intestinal integrity, nutrient absorption, and the development of the host's innate and adaptive immune system (Diaz Heijtz et al., 2011). The balanced gut microbiome, also known as *symbiosis*, is associated with the healthy state of an individual whereas *dysbiosis* which means disruption of this balance is associated with a diseased state.

#### 2.1.2 *Clostridium celatum* in the human gut

Four major microbial phyla: *Firmicutes*, *Bacteroides*, *Proteobacteria*, and *Actinobacteria* constitute 98% of the human gut microbiota and *Clostridia*, belonging to phylum *Firmicutes*, comprises one of the most abundant bacterial classes (Lopetuso et al., 2013). Genus *Clostridium* makes up anywhere from 0 to 42 % of all the reads in the human gut (McDonald et al., 2018). *Clostridium* species predominate in the large intestine and colonizes especially in the colon (Guo et al., 2020).

*Clostridium celatum*, the species used in our study, was first isolated from human feces in 1974 and it was identified as gram-positive anaerobic bacterium and non-toxic (Hauschild & Holdeman, 1974). There was no association of *C. celatum* with any human infection, until in 2015, two cases of infection with the bacterium were reported in a) a 53-year-old man with gallbladder removed, and b) an 87-year-old woman with a history of osteoporosis and knee arthrosis (Agergaard et al., 2016).

### 2.1.3 The gut microbiota-brain axis

Gut dysbiosis has been associated with brain development in mice models (Diaz Heijtz et al., 2011). For example, infection with *Campylobacter jejuni*, a food-borne pathogen, enhances anxiety-like behavior in mice (Goehler et al., 2008) and rats infected with *E. coli* neonatally experienced memory impairment in adulthood (Bilbo et al., 2005). Researchers have demonstrated that normal gut microbiota can impact brain functioning and behavior in mice as well (Diaz Heijtz et al., 2011).

Gut dysbiosis has also directly been associated with multiple neurological disorders in humans, and it has been emphasized because of its association with Autism Spectrum Disorder (ASD). Many studies have reported GI abnormalities such as increased intestinal permeability and altered composition of the gut microbiota in ASD individuals (Hsiao, 2014). In 2013, using a MIA (Maternal Immune Activation) mouse model which is known to display ASD symptoms (Malkova et al., 2012), Hsiao et.al demonstrated that augmentation with *Bacteroides fragilis* altered gut microbiota and blood metabolite profiles, corrected gut permeability issues and ameliorated ASD-associated communicative, social, repetitive and anxiety-like behavioral symptoms (Hsiao et al., 2013). An open-label clinical trial evaluated the impact of Microbiota Transfer Therapy on GI and ASD symptoms of 18 ASD-diagnosed children. GI symptoms were reduced by 80% and there was a significant improvement in behavioral ASD symptoms (Kang et al., 2017). 2 years later, they did a follow-up study on the same participants and confirmed that the improvement in GI symptoms was maintained and behavioral ASD symptoms improved even more after two years of the treatment (Kang et al., 2019).

Here, we tested the hypothesis that *C. celatum* can negatively impact the anxiogenic phenotype in a mice model. We focused on *C. celatum* because it is a non-pathogenic bacteria (BSL-1), part of normal gut flora of humans and mice, and was found to be enriched in children with Autism in a crowdsourced study (David et al., n.d.). Significantly elevated levels of *Clostridium* species have also been reported in other autism-related studies (Angelis et al., 2013; Finegold et al., 2002)

## 2.2 Enteroendocrine cells (EECs), vagal nerve, and the gut microbiome

### 2.2.1 Enteroendocrine cells in the gut

The gut has been described as the largest endocrine organ of the body, because of its ability to sense nutrients and bacterial metabolites and produce over thirty different hormones.

Enteroendocrine cells (EECs) constitute sensory cells of the gut and produce the majority of the gut hormones (Gunawardene et al., 2011). EECs comprise only 1% of the total gut epithelial cells, and still, the gut forms the largest endocrine system in the human body, both in terms of the number of endocrine cells and number of hormones (Rehfeld, 1998).

EECs are typically triangular or flask-shaped and depending on their position in the GI mucosa, they are classified into *open-type* if their apical surface is exposed to the gut lumen and *closed-type* if they don't come into contact with gut lumen, as shown in Figure 1 (Liddle, 2019).

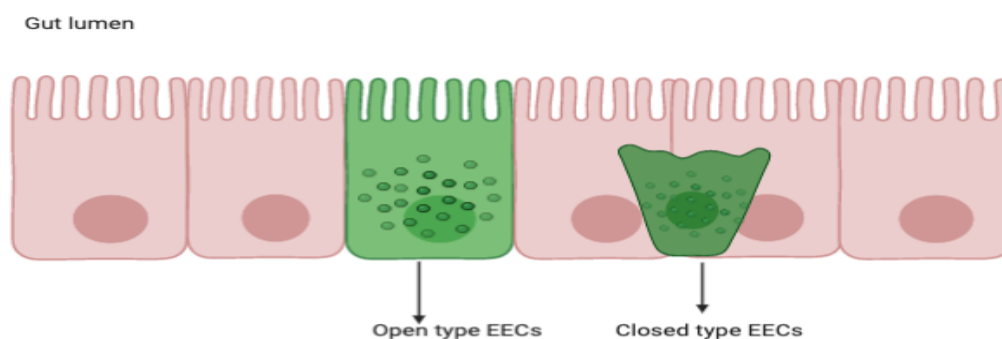


**Figure 1:** Open and closed type of EECs

### 2.2.2 Different types of EECs

EECs are also known as “*specialized trans-epithelial signal transduction conduits*” which sense luminal nutrients and other stimuli and respond by secreting a variety of peptides which depends on their location in the gut (Worthington et al., 2018). On the basis of their location and the peptide secreted, they are divided into many sub-populations as shown in Figure 2. Earlier it was thought that one cell type produces only one type of hormone but this hypothesis has been refuted and it has been proved that there is coexpression of different types of hormones by one cell type (Gribble & Reimann, 2016).

As can be seen in Figure 2, G cells in the stomach mainly produce gastrin that controls gastric acid secretion. They do so by acting on another EEC population in the stomach: entero-chromaffin cells (ECCs) that secretes histamine which functions by activating parietal cells to secrete gastric acid. Somatostatin producing D cells in the intestine and pancreatic islets inhibit gastric acid secretion. A-type cells in the stomach regulate appetite by producing ghrelin. K cells that produce GIP (Glucose dependent insulinotropic polypeptide) and I cells which produce cholecystokinin (CCK) are located in the proximal small intestine, whereas L cells producing PYY (Peptide YY) and glucagon-like peptides (GLPs) are present in the distal small intestine and colon. There are other types of ECCs that produce serotonin known to exert paracrine effects in the GI tract and thus, promotes intestinal motility (Liddle, 2019).

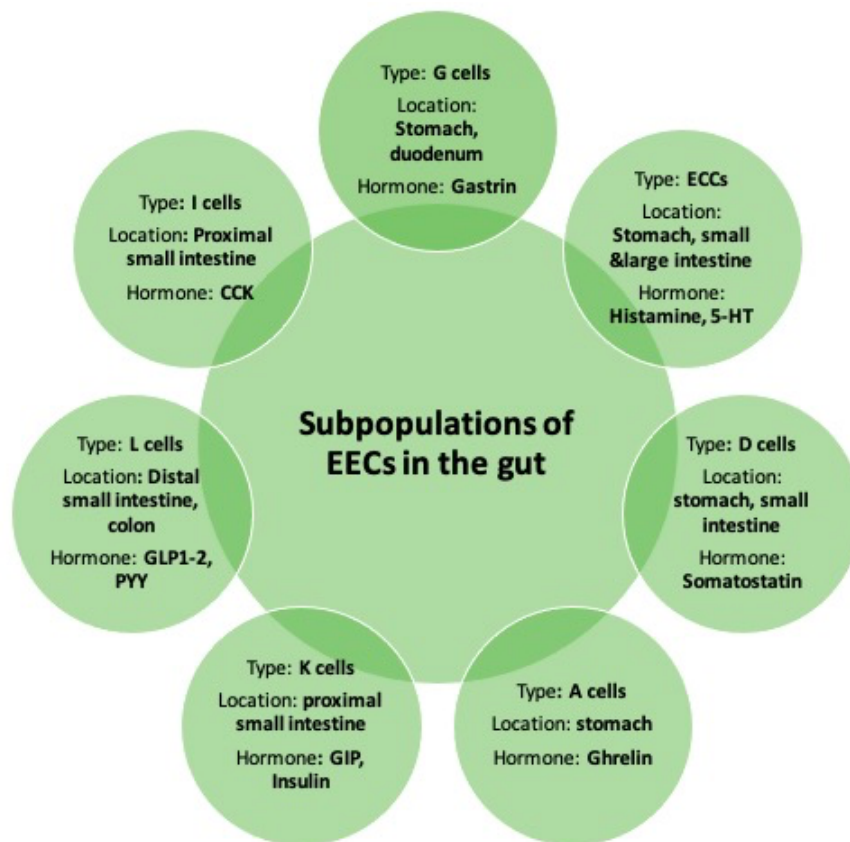


**Figure 2:** Different types and location of EECs in the Gastrointestinal Tract (adapted from (Latorre et al., 2016))

### 2.2.3 Chemosensation by EECs

On the basis of the fact that the open-type EECs extends from lumen to basal lamina, as seen in Figure 1, they are regarded as chemosensors, capable of sensing luminal contents and release secretory products accumulated in secretory granules into the basal lamina where they act either locally or on distant targets by entering the bloodstream (Sternini et al., 2008). They can also act on vagal afferent fibers, which are present in close proximity to the intestinal epithelium, thus forming an important component of the gut-brain axis (Moran et al., 2008).

The luminal content that is sensed by sensory receptors on EECs include glucose, peptides, amino acids and fatty acids, for example, G-protein coupled receptors (GPCRs) present on the surface of L type EECs sense glucose in lumen and release glucagon-like polypeptide-1 (GLP-1) through a mechanism involving an increased influx of  $Ca^{2+}$  (Feher, 2017).

### 2.2.4 Neuropods discovered in EECs

It has recently been recognized that many EECs possess basal processes known as neuropods that not only contain hormones but also form synaptic connections with nerves (Liddle, 2019). The earliest evidence of basal processes in EECs is in 1979 when researchers demonstrated that rat and human D cells (somatostatin producing EECs, see Figure 2) have long cytoplasmic processes that come in contact with distant gastrin cells present in the same zone, thus providing evidence for paracrine functioning of these cells (Larsson et al., 1979). Similar processes have also been observed in L cells (PYY producing EECs, see Figure 2) (Lundberg et al., 1982). While these basal processes are more prominent in D and L-type EECs, short basal processes have also been observed in CCK producing EECs (I cells, Figure 2) (Chandra et al., 2010).

Several unique features of the process were revealed later using PYY-GFP transgenic mice (Bohórquez et al., 2011). First, mitochondria and secretory vesicles were present in high concentrations in this cytoplasmic process. Second, the process contained neurofilaments, the structural component of neuronal axons. Finally, there was a physical connection between this process and the enteric glia (Figure 3). These features indicated that EECs have neuron-like properties and they named these axon-like processes as *neuropods* (Bohórquez et al., 2014).

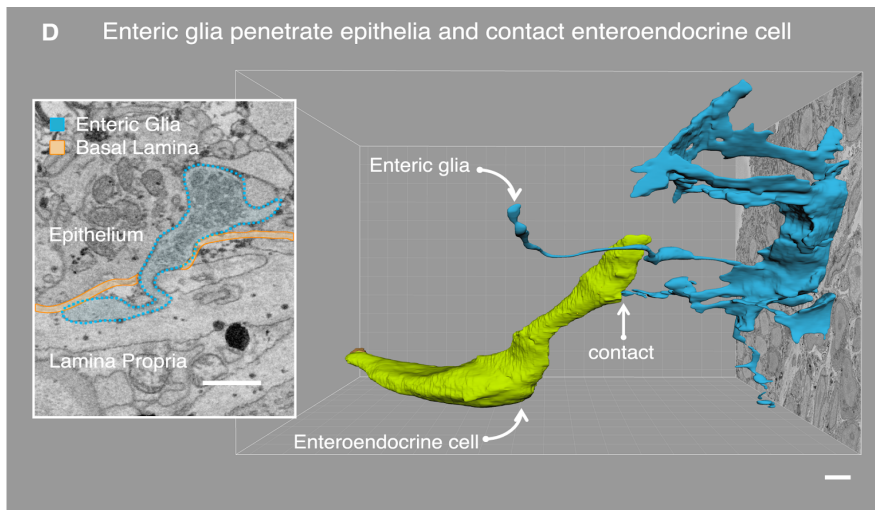


**Figure 3 :** Enteric-glia and EECs connection (Bohórquez et al., 2014)

### 2.2.5 EECs connection with neurons via neuropods

In 2015, they found a connection between neuropods and CGRP (calcitonin gene-related peptide) nerves, which have been described as markers of sensory neurons. They recapitulated the connection in vitro by co-culturing EECs isolated from CCK mice and sensory neurons from the trigeminal or dorsal root ganglia of the wild type mouse. As can be seen in Figure 4, the neuron extended a small neurite towards EEC and EEC responded by elongating the cytoplasmic process towards the neuron. These results indicate that EECs and neurons have an affinity towards each other (Bohórquez et al., 2015).



**Figure 4:** Connection of a single CCK-GFP EEC (green) isolated by FACS, with a sensory neuron (Dil-labeled, red), imaged using fluorescence incubator microscope (Bohórquez et al., 2015)

Further, on the basis that EECs contained synaptic vesicles that are essential for neurotransmission, and they expressed many pre, post, and trans-synaptic genes, the connection between EECs and neurons appeared to be a synapse. The synaptic connection was proven *in vivo* using the monosynaptic rabies virus neuron tracing experiment. The delivery of this virus into the colon lumen resulted in the infection of mucosal nerves, indicating that EECs connected to neurons through a synapse (Bohórquez et al., 2015).

*These studies provided direct evidence that the neuropods of I and L cells have synaptic features and they form synaptic connections with nerves innervating the gut, thus forming a neuroepithelial circuit.*

#### *2.2.6 Neural circuit between EECs and the brain via vagus nerve*

In 2017, researchers showed that purified CCK expressing EECs contact Pgp9.5 sensory nerve fibers and express presynaptic protein synapsin-1 and synaptic adhesion genes. By using a monosynaptic rabies virus, they determined the source of the nerves synapsing with EECs. They found that these EECs communicate with nerves in the vagal nodose ganglia and this neural circuit connects the brain to the gut lumen in a single synapse. They recapitulated this neural circuit in-vitro by co-culturing vagal nodose neurons and intestinal organoids. They also tested the function of the circuit by co-culturing vagal neurons and purified EECs and performing whole-cell patch-clamp recording to record response to the sugar stimulus which was transduced from gut lumen to brain via EECs in milliseconds. By using fluorescent reporter iGluSnFR, they revealed that EECs use neurotransmitter glutamate to transduce fast sensory signals to vagal neurons (Kaelberer et al., 2018).

*This indicated that the CCK producing EECs (I cells) connect to the brain through a single synapse, and neurotransmitter glutamate, contained in the small, clear (yellow) secretory vesicles in the neuropods (see Figure 5) is involved in this connection, whereas the peptide hormone CCK, contained in large, dense (blue) vesicles are released locally and works in a paracrine fashion by acting on neighboring cells or local nerves (Liddle, 2019).*

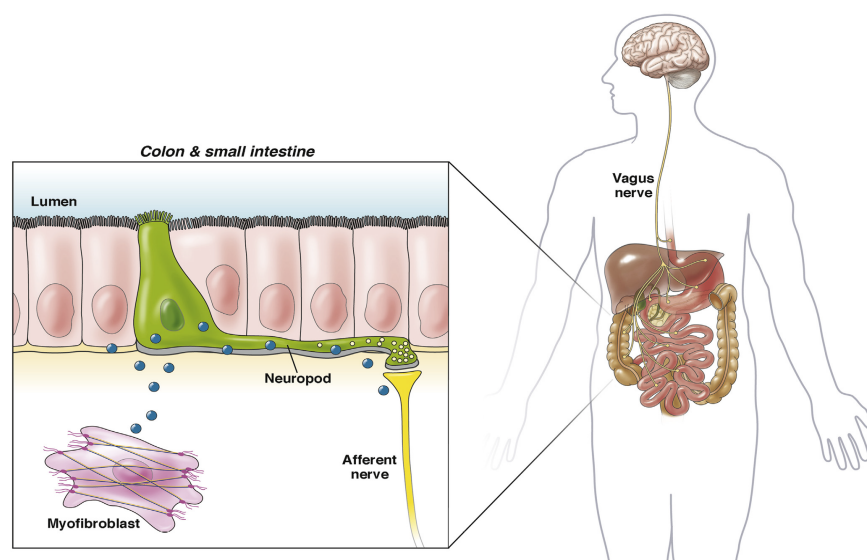


**Figure 5:** Enteroendocrine cell communication in the gut (Liddle, 2019)

### 2.2.7 Interactions between gut microbiome and EECs

The host-microbe communication is mediated by the gut, especially sensory epithelial cells (EECs) present in the intestine. It has been well established that EECs can sense nutrients such as glucose and transmit the signals to brain via vagus nerve (Kaelberer et al., 2018), but whether they can be directly stimulated by the gut microbiome is still being explored. Here, we wish to understand whether *C. celatum* and other taxa in the gut microbiome modulate the brain activity through direct interaction with EECs.

Recently, researchers using zebrafish model, discovered that the bacteria *Edwardsiella tarda* activates EECs through Trpa1 receptor on EECs, which is “an excitatory calcium-permeable non-selective cation channel” and promotes intestinal motility by activating enteric motor neurons and ultimately activating vagal network (Ye et al., 2020). It would be interesting to know if the other members of the gut microbiome can directly interact with EECs and if this is the mechanism by which the gut relays information to the brain. To understand the interactions between the gut microbiome and the EECs, we are using a technique called “Whole Cell Cross-Linking” which has been used to identify novel protein-protein interactions. The technique is based on covalently cross-linking two proteins within 9-12 Å. This strategy has been

used and validated to discover receptor/ligand pairs that mediate host-microbes association. It is applicable to any host-microbe interaction which is mediated by protein-protein interactions and is valuable in understanding how the microbes interact with the host that leads to uncover potential drug targets, vaccine development and pathogenesis mechanisms (Weimer et al., 2018).

We cross-linked these EECs with *C. celatum* and other gut microbiota using “cell impermeable cross-linking reagent- Sulfo-N-hydroxysuccinimidyl-2-(6-[biotinamido]-2-(p-azido benzamido)-hexanoamido) ethyl-1,3'-dithiopropionate (Sulfo-SBED)” (Das & Fox, 1979) (Sulfo-SBED Biotin Label Transfer Reagent, n.d.). Sulfo-SBED contains biotin, which is transferable to the interacting protein, due to which it's also used as “label transfer reagent.” A sulfo-NHS ester group of Sulfo-SBED reacts with primary amines to form covalent amide bonds, and an aryl-azide moiety which is UV-light activatable, upon photolysis, form nitrenes by reacting with nucleophiles, especially amines and thus captures the interacting protein.

### 3. Materials and Methods

#### 3.1 Comparative and phylogenetic analysis of *C. celatum* genome

After BLAST of 16S rRNA gene of *C. celatum* against the NCBI Complete Prokaryote Genome Database (refseq and genbank genomes)- took all the genomes with percent identity more than 94.5%, resulting in 326 genomes (after removing the multiple contigs from the same genome). Further analysis was continued with the species whose complete genomes could be found in the IMG database. We ended up with 248 genomes, downloaded their KO abundance data and further analysis was done in R (version 4.0.3). Significant different KOs was found on the basis of p-value (significance level 0.05)

All the 248 genomes were searched in the Pathosystems Resource Integration Center (PATRIC) database for the presence of virulence factor. In addition, previously published literature data was used to determine their pathogenicity. *C. celatum* was considered a potential pathogen for the analysis on the basis of a recent report where 2 cases of infection in old and immunocompromised people with *C. celatum* have been documented (Agergaard et al., 2016).

**Table 1:** Pathogenicity designations used for the comparative analysis of *C. celatum* genome

Pathogenicity	Meaning
No	Established non-pathogen
No without VF	No literature on it's pathogenicity and no VF present in PATRIC
No with VF	No literature on it's pathogenicity but VF is present in PATRIC
Unknown	No literature and genome not found on PATRIC
Potential	Literature on it's potential pathogenicity
Yes	Established pathogen

After downloading the 16S rRNA sequences of these 248 genomes from the IMG database, a phylogenetic tree was constructed using the general time reversible (GTR) model to understand the similarities between *C. celatum* and other *Clostridium* genomes. *Methanococcus voltae* A3 was used to root the tree.

### **3.2 Growing *Clostridium celatum* in anaerobic chamber**

*Clostridium celatum* DSM 1785 was grown for 48 hours in Carbohydrates chopped Media (Anaerobic systems) at 37C in Anaerobic Chamber (Bactron, Sheldon Manufacturing, Inc) under supply of an anaerobic gas mixture (AMG contains 5% CO<sub>2</sub>, 5% H<sub>2</sub>, and 90% N<sub>2</sub> ). To prepare the sample to feed mice, liquid *Clostridium celatum* cultures were centrifuged at 3000 rpm for 5 minutes and resuspended in apple juice. We also measured the bacterial concentration in the samples using a spectrophotometer, to keep the concentration consistent throughout the study.

### **3.3 Animals**

#### *3.3.1 C57BL/6 mice*

Mice were housed, bred and fed in the Oregon State University animal facilities at Laboratory Animal Resources Center (LARC). Female mice, at postnatal day 12.5 of pregnancy, were injected with either polyinosinic:polycytidylic acid (Poly-IC) to stimulate maternal immune system to generate PolyIC testing mice displaying autistic symptoms (Malkova et al., 2012) or with NaCl to generate control mice. After the pups were born and weaned, they were randomly divided into groups to receive either the normal apple juice(AJ) or the apple juice containing *Clostridium celatum*. At last, we have 4 different groups as shown in Figure 6. Mice were fed for 4 weeks (3 times a week) after weaning and then underwent behavior testing. Ultimately the animals were sacrificed and their tissues- spleen, liver, brain and gut contents from duodenum, jejunum, ileum, caecum and colon were collected for sequencing.

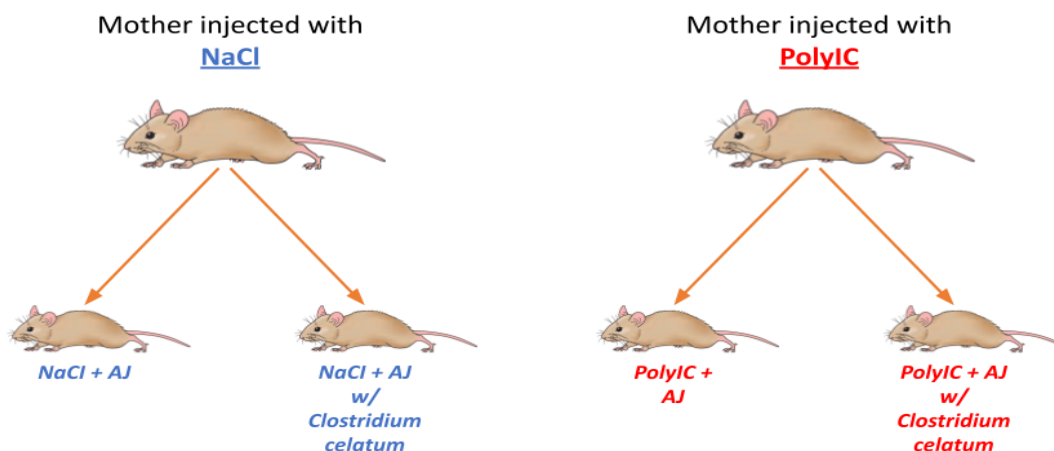


**Figure 6:** Four different types of treatment groups for mice for the study. NaCl = Sodium Chloride injected mouse, AJ= Apple Juice, PolyIC- PolyIC injected mouse

### 3.3.2 CCK-GFP mice colony establishment and management

The CCK-GFP mice for the second part of the project have GFP labeled EECs, which can be isolated from other intestinal epithelial cells (non-GFP) using Fluorescent Activated Cell Sorting. The genotype of this mouse is modified to contain multiple copies of a modified bacterial artificial chromosome (BAC) in which enhanced GFP (EGFP) fluorescent reporter gene is inserted upstream of the coding sequence of the targeted gene Cck, which is present in the EECs and thus have GFP labeled EECs.

2 breeding pairs of CCK-GFP positive mice (Swiss Webster- strain 000249-MU) were imported from the Duke University (courtesy of Prof. Rodger Liddle) after a MTA (Material Transfer Agreement) with MMRRC. Mice were housed in Oregon State University animal facilities at Laboratory Animal Resources Center (LARC). They were foster rederived for *Helicobacter* in quarantine for about 10 weeks. After their successful rederivation, we set up the breeding pairs to establish and maintain the mice colony. To create in-house CCK-transgenic mice colony, we also bred the CCK-GFP (+) mice with Swiss Webster (SWR/J) mice, ordered from Jackson Laboratory.

### 3.4 Viability of *C. celatum* in apple juice

After centrifugation of liquid *C. celatum* cultures in Carbohydrates media at 3000 rpm for 5 minutes and resuspending in apple juice, we incubated the *C. celatum* in apple juice in falcon tube outside the anaerobic chamber at room temp for 48 hours to check it's oxygen toxicity and confirm its viability. After 0 minute, 30 minutes, 1 hour, 2 hour, 3 hours, 24 hours, 48 hours, 150 ul of the bacterial culture was spread on Red Blood agar plates and the plates were incubated in anaerobic chamber at 37C. After 48 hours, the colonies on the surface of the plates were counted for each time interval and colony forming unit (CFU/ml) was estimated according to the following formula:

$$\text{CFU} = \text{no. of colonies} \times \text{dilution factor} / \text{volume of culture plated}$$

### 3.5 Behavior tests

After feeding the mice for 4 weeks with either normal apple juice or *Clostridium celatum* in Apple juice, following behavior tests were performed. Mice were habituated to the behavior testing room for 30 minutes before starting each test.

#### 3.5.1 Open Field Habituation test

This test monitors the anxiety-like behavior which is considered to be reduced after repeated exposure to the increasingly familiar environment. After 30 minutes of habituation to the room, mice were placed individually in an open plastic bin, enclosed by four walls for 5 minutes for 3 consecutive days. The movement of the mice was tracked by AnyMaze software to determine the time spent per entry to the center of the arena, which is a measure of anxiety. We also measured the total distance as the measure of exploratory behavior and non-associative learning following habituation (Bolivar, 2009).

#### 3.5.2 Elevated Plus Maze

This test is based on the conflict between the natural disinclination of mice for open and elevated spaces and their exploratory behavior in novel environments. Mice were placed in the center of a plus-shaped maze, which is elevated off the ground and consists of two open arms facing each

other and two arms enclosed by walls. Movement of mice was recorded for 5 minutes. The amount of time spent in the open arms was measured which is indicative of anxiety, considering the natural tendency of mice for the secured sections of maze, i.e. closed arms.

### *3.5.3 Marble Burying*

This test measures the anxiety-like and repetitive behavior of mice. Mice exhibit digging behavior in response to new environments. Mice were placed in new cages with wooden bedding and 15 marbles arranged in 3 rows of 5, on top of the bedding, for 30 minutes. At the end, the number of marbles untouched, moved or buried were counted.

### *3.5.4 Three Chambered Sociability and Social Novelty Test*

This test involves 3 stages: Stage 1 in which testing mice was placed in the middle chamber to habituate to the apparatus for 5 minutes. Stage 2 in which a novel mouse was placed in a cage in one of the side chambers, an empty cage in the other side chamber and the testing mouse was placed in the center. Testing mouse was given the opportunity to interact with this novel mouse and novel object for 10 minutes. Here, the mouse was tested for “sociability”, if it prefers to interact with a novel mouse over a novel object. In the final stage, the novel mouse used in stage 2 was moved to the third chamber, and a new novel mouse was placed in the old chamber. Testing mouse was placed in the center and was allowed to interact with both the mice for 10 minutes to determine the “social novelty” of the testing mouse. The movement of the mouse was tracked throughout by AnyMaze software and time in each of the side chambers was measured to determine sociability and social novelty.

## **3.6 Genotyping of CCK-GFP mice**

### *3.6.1 DNA extraction*

DNA from mice ear punches or mice hair was extracted using DirectPCR Lysis Reagent(Ear) with the minor modifications in the protocol provided with the reagent. Proteinase K solution was added to the DirectPCR reagent (with final concentration of 0.5 mg/ml) to make the extraction solution. 200 ul of this solution was added to each tube containing the ear tissue for

cell lysis. Following this, the crude lysates were incubated at 85C for 45 minutes in the water bath to inactivate proteinase K. 1 ul of the crude lysate was used for the PCR for ear samples and 2 ul of the crude lysate was used for hair samples.

### 3.6.2 PCR setup

PCR parameters were set up according to the MMRRC 249 genotyping protocol, with few modifications.

**Table 2:** PCR master mix components for CCK-GFP mice genotyping

Component	Volume/ sample
Go-Taq green master mix	12.5 ul
(Cck) F primer	0.5 ul
GFP Rev primer	0.5 ul
DNA template	1 ul for ear samples/ 2 ul for hair samples
Molecular grade water	5.5 ul

(Cck) F primer sequence: 5'- TAG GAA CTT CGC TTG GCT ACG G -3'

GFP Rev primer sequence: 5'- TAG CGG CTG AAG CAC TGC A -3'

Thermocycler settings: Lid temperature 95C

1. 95C 5 minutes
2. 94C 30 seconds
3. 65C 30 seconds
4. 72C 30 seconds
5. Repeat steps 2-4 34 times for a total of 35 cycles
6. 72C 7 minutes
7. 4C hold until refrigerate product

### 3.6.3 Product Analysis

3% agarose gel with Sybr Gold staining was prepared and the PCR products were analysed at 100 V for 30 minutes. A DNA ladder of 10 kb was used to examine the expected product at 374 bp.

### 3.7 Magnetic sorting of EECs

After measuring cell viability, the single cell suspension was centrifuged at 800 rpm. After removing the supernatant, the cell suspension was labeled with 100 ul of Antibody solution (10 ul of PE-conjugated claudin-4 antibody in 90 ul of separation buffer) by incubating in dark at 4C. Cells were washed with labeling buffer (PBS + 2mM EDTA) to remove any unbound antibody. For flow cytometry analysis, cells were resuspended in the separation buffer and analysed in a flow cytometer.

To magnetically isolate the cells, they were resuspended in the labeling buffer and incubated with 10 ul of Anti-PE microbeads. Cells were washed with a separation buffer (MACS BSA stock solution diluted 1:20 with autoMACS Rinsing solution) after centrifugation at 800 rpm. This suspension was applied onto a magnetic column placed in the magnetic field of a suitable MACS separator. Unlabeled cells that passed through were also collected and labeled cells were collected by adding the separation buffer and firmly pushing the plunger onto the column.

### 3.8 EECs culturing

It involves 4 major steps: dissection of the mice intestine, mechanical and enzymatic dissociation of the intestine to get individual cells, sorting of the EECs from all the intestinal epithelial cells and their plating on matrigel coated plates (Kaelberer et al., 2018).

*Tissue acquisition:* After euthanizing the CCK-GFP mice using isoflurane, the proximal half of the small intestine was dissected. The intestine was cut lengthwise and into small sections.

*Dissociation:* After removing the PBS, the tissue was incubated with Dissociation Reagent 1 (EDTA in DPBS) at 4C and then at 37C. After removing the Dissociation Reagent 1, cold PBS

was added and villi and crypts were mechanically detached and collected through 100 um filters. This step was repeated for 4-5 times. The crypts and villi were centrifuged at 800 rpm and then incubated with Dissociation Reagent 2 (Dispase and Collagenase) for 15 minutes at 37C. Cells were spun down again and resuspended in complete L-15 medium (containing HEPES buffer, FBS, Pen-Strep) and DNase to avoid cell clumping. Cells were filtered through a 70 um and then a 40 um filter and centrifuged again to isolate single cells. After resuspending in complete L-15 medium, cell viability and cell concentration was measured using Trypan blue assay, which stains the dead cells blue and live cells are unstained.

*Separation and Purification:* Cells were sorted using Fluorescent Activated Cell Sorting (Sony SH800 cell sorter) selecting for GFP fluorescent cells. Cells were collected in complete DMEM media listed below.

*Plating and incubation:* Sorted cells were plated on matrigel coated plates. Complete DMEM media (DMEM containing Glutamax, HEPES, B-27, Anti-Anti, N2, NAS, Spondin, Noggin, NGF, EGF) was used as culture medium and plates were placed in an incubator (37C, 5% CO<sub>2</sub>) overnight.

### **3.9 Neurons culturing from nodose ganglion**

After euthanizing the mouse using isoflurane and decapitation, the nodose ganglion was anatomically dissected and immediately placed in a tube with L-15 media on ice. After washing once with PBS, 1 ml of L-15 media was added and then it was incubated with Liberase digestion enzyme at 37C for 1 hour. After removing the Liberase media and twice washing with PBS, fresh media was added. The ganglion was mechanically dissociated by titrating with pipette to get individual cells. After passing through the 70 um filter, the cells were ready to be plated.

### **3.10 EECs and neurons co-culturing**

To recapitulate the connection between the EECs and the nodose neurons, they were plated in the same dish and visualized after 24 hours and 48 hours to check if there is any connection formed between EECs and neurons.

### **3.11 EECs cross-linking with gut microbiota**

#### *3.11.1 EECs culturing and store gut contents*

CCK-GFP mouse was sacrificed and its proximal half small intestine was dissected. The gut contents were collected and stored in Tyrode's buffer overnight and the same tissue was dissociated to isolate and grow EECs overnight on matrigel coated plates.

#### *3.11.2 Bacterial labeling and cross-linking with EECs*

Gut contents in the Tyrode's buffer were filtered through a 100 um and 40 um filter. Total protein content in the bacterial suspension was determined through a Bicinchoninic Acid (BCA) assay. Sulfo-SBED was added to bacterial suspension to label the bacteria. After incubation in dark, on ice for 45 minutes, glycine was added to quench the labeling reaction. To remove the unreacted reagent, bacteria was washed twice with Tyrode's buffer. 1 ml of labeled bacteria was added to the dish with EECs grown overnight in the ratio of 1000 :1 and incubated at 37C for 60 minutes. Then, after removing and collecting the supernatant (which contains the non-interacting bacteria), the interacting bacteria and EECs in the dish were placed under UV for 4 minutes to form the covalent bonds for cross-linking the bacteria and EECs. The cross-linked bacteria and EECs were mechanically detached from the surface of the plate and stored in the microcentrifuge tube for DNA extraction and subsequently 16S PCR and sequencing for further analysis.

#### *3.11.3 DNA extraction from the cross-linked cells*

100 ul of each cross-linked sample was boiled in a water bath for 5 minutes. The extraction solution was prepared by mixing 2.5 ul Proteinase K solution and 100 ul DirectPCR Reagent (diluted 10 times for a small number of cells). 100 ul of the extraction solution was added to each sample and incubated at 85C for 20 minutes in a water bath to inactivate the Proteinase K. 10ul/3ul of the crude lysate was used for the PCR, depending on the number of cells.

#### *3.11.4 16S rRNA amplification and sequencing*

The V4 region of the 16S rRNA gene was amplified and sequenced according to the protocol described by the Earth Microbiome Project.

**Table 3:** 16S PCR master mix components

<b>Component</b>	<b>Volume/ sample</b>
PCR master mix (2x)	10 ul
Forward primer	0.5 ul
Reverse primer	0.5 ul
DNA template	10 ul/3ul
Molecular grade water	13 ul

Primers: 16S V4 515F–806

#### Cycle settings

1. Lid temperature: 95C
2. 94C 3 minutes
3. 94C 45 seconds
4. 50C 60 seconds
5. 72C 90 seconds
6. Repeat steps 2-4 34 times for a total of 35 cycles
7. 72C 10 minutes
8. 4C hold until refrigerate product

The amplified products were sequenced on an Illumina MiSeq sequencer and the 16S data was processed using DADA2. All the other analyses were performed in R.

**Table 4:** Different types of amendments/samples used in crosslinking data analysis

<b>Amendment/Samples</b>	<b>Meaning</b>
AD (After Dilution)	Diluted bacteria added to plates(EECs) for crosslinking
BW (Bacterial Wash)	Sample taken after incubating bacteria w/ cells, before UV (cells not interacting with EECs removed)
Xlink (Cross link)	Sample taken after cross-linking cells w/ UV

## 4. Results

### 4.1 *Clostridium celatum* in the gut-brain axis

#### 4.1.1 Comparative genomic and phylogenetic analysis of *C. celatum*

This work focuses on *Clostridium celatum*, a *clostridium* species found associated with autism. As indicated in the literature review, *C. celatum* was originally isolated from normal human feces and was non pathogenic (Hauschild & Holdeman, 1974). But in 2016, over 40 years after its discovery, two reports described *C. celatum* as potentially pathogenic. To gain better understanding of its genomic features and any potential pathogenic features, we extracted the Kegg Orthologs (KO) of 248 *Clostridium* genomes (each KO representing a characterised functional gene), closely related to *C. celatum* (94.5% similarity, BLAST). This resulted in a concatenated matrix with over 20,000 KOs, and we filtered out the KOs that were present across all genomes, resulting in 1089 KOs. We overlaid the pathogenicity status of each *clostridium* strain in a constrained Principal Coordinate analysis (PCoA) plot showing Bray–Curtis distances between the selected KOs in Figure 7. This analysis shows clear separation of *C. celatum* from the pathogenic *Clostridium* species and indicates that it shares similarities with the other potential pathogen *C. tarantellae* DSM 3997, which was confirmed by a permanova test (p-value < 2.2e-16) for separation between group on the ordination.

To further our analysis, we also constructed a phylogenetic tree (Figure 8) using full length 16S rRNA genes of all the considered genomes. We can observe that *C. celatum* is closely related to *Clostridium beijerinckii* DJ149 and *Clostridium saccharobutylicum* DJ276, both of them are not pathogens and no virulence factor is present in the PATRIC database.

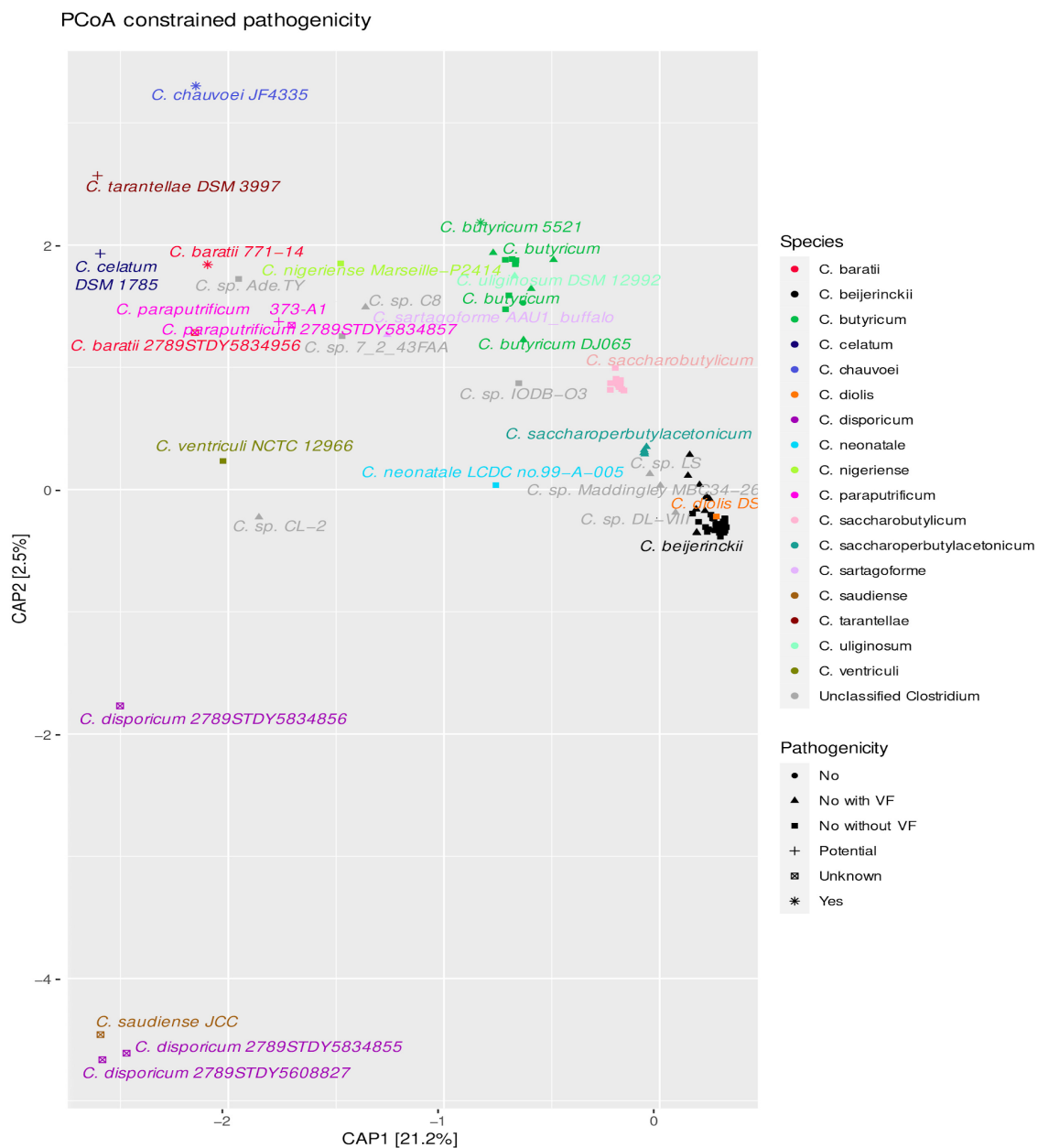


**Figure 7:** Constrained Principal Coordinate analysis (PCoA) plot of Bray–Curtis distances between selected KEGG Orthologs of *Clostridium celatum* and closely related *Clostridium*. The PcoA was constrained by pathogenicity.

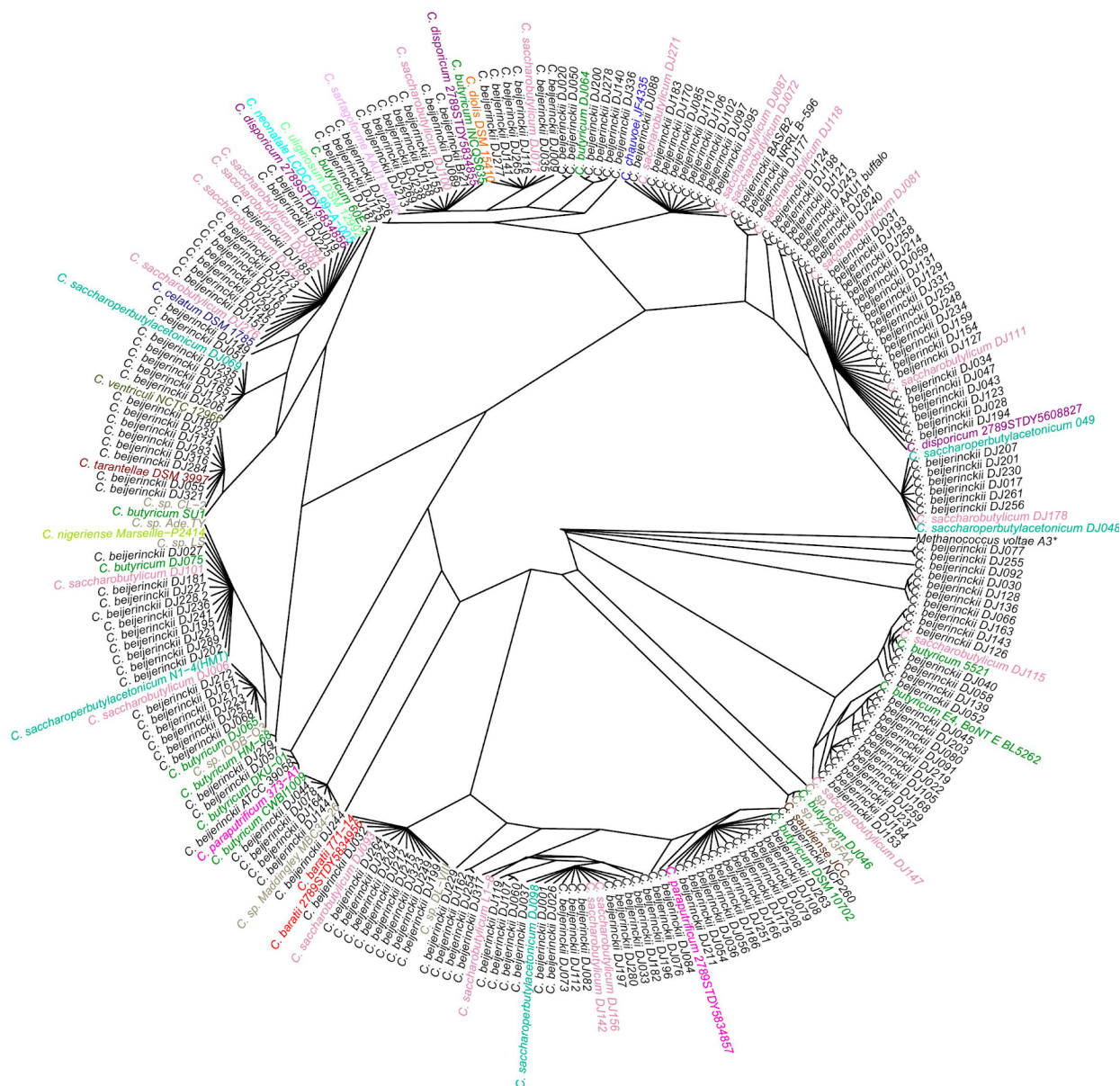


**Figure 8:** Phylogenetic tree of 248 *Clostridium* genomes based on full length 16S rRNA. Here, *Methanococcus voltae* A3 is used as an outgroup to root the tree.

#### 4.1.2 Viability of *C. celatum* in apple juice

In order to test if *C. celatum* could negatively impact the behavior phenotypes, we fed C57BL/6 mice with either apple juice or apple juice containing *C. celatum* (Figure 5) for 4 weeks before they underwent behavioral tests. They were fed three times a week, in order to maintain a constant bacterial colonization in the original microbiota. *Clostridium celatum* is grown in

anaerobic chamber but fed in apple juice to the mice: the goal of this experiment was to test the viability of *C. celatum* in apple juice during and after its transfer to the mice. We checked the viability of *C. celatum* in apple juice at different time intervals. The estimate of CFU/ml, which is a measure of viable bacterial cells, was calculated as: no.of colonies X dilution factor /volume of culture plated. CFU/ml at each time interval is indicated in Table 5 and Figure 9. The viability of *C. celatum* dropped after some time, but the CFU/ml after 48 hours is maintained to almost half the starting CFU/ml ~ 2000 CFU/ml, which supports our feeding design of feeding the mice after every 48 hours. Note that we did not plate the number of cells that were viable and present in the original growing media.

**Table 5 :** CFU/ml of *C. celatum* in apple juice at various time intervals

Time interval	T1-CFU/ml	T2- CFU/ml
0 minute	3173	3812
30 minutes	4203	4427
1 hour	3546	3279
2 hours	2213	3973
3 hours	2013	3546
24 hours	2106	4186
48 hours	2053	1906

T1 is the count for 1 set of plates and T2 is the count for the other set of plates.

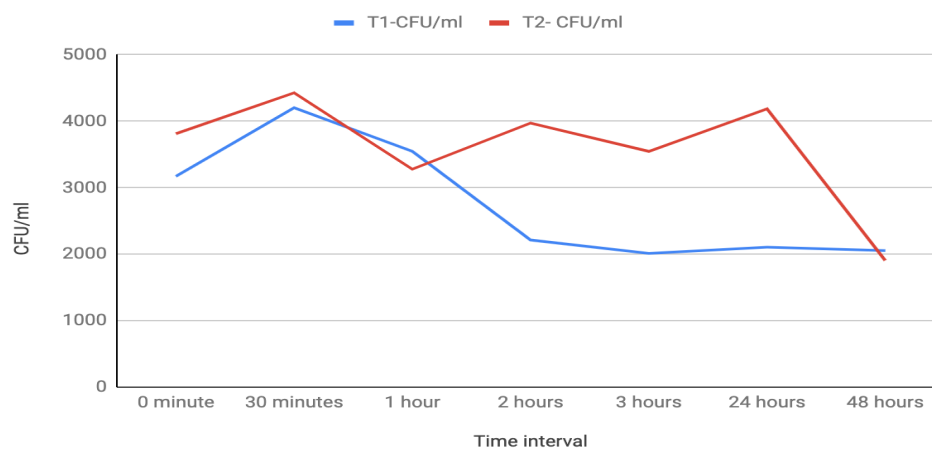


**Figure 9:** Viability of *C. celatum* culture in apple juice over a period of 48 hours. The red line represents the T1 set of plates and the blue line represents the T2 set of plates.

#### 4.1.3 Open Field Habituation test

C57BL/6 mice were fed either apple juice or apple juice containing *C. celatum* (Figure 5) for 4 weeks before they underwent behavioral tests. They underwent open field habituation test which is performed to assess exploratory, non-associative and locomotor activity of the mice. The mice were placed in the center of the apparatus and the movement of the mice was tracked. The software tracked the time (ambulatory or not), speed and distance in the whole apparatus and in the center zone. Measures such as time per entry in the center, or the total distance explored were used as a proxy for anxiogenic phenotype based on the mouse aversion to open space, and the total distance as reduction of the exploration behavior following habituation (Bolivar, 2009).

As seen in Figure 10, saline injected, apple juice fed mice (NaCl-AJ) spent more time exploring on Day 3 compared to Day 1 (p value = 0.067, wilcox test) and Day 2 (p value = 0.12, wilcox test), showing that our control group seemed to habituate to the arena over the three days. On the other hand, saline injected mice who were fed *C. celatum* (NaCl-Bact) did not display change between day 1 and 3, showing a lack of habituation, revealing possibly a more anxious phenotype. PolyIC injected mice who were fed apple juice with and without *C. celatum* (PolyIC-AJ and PolyIC-Bact) didn't spend significantly more time on Day 2 and Day 3 as compared to Day 1 (p value > 0.15, wilcox test). A repeated ANOVA was also calculated and the effect of 'Day' (p-value= 0.021) and "Treatment" (p-value = 0.004) was found to be significant on the time spent per entry to the center area of the chamber.

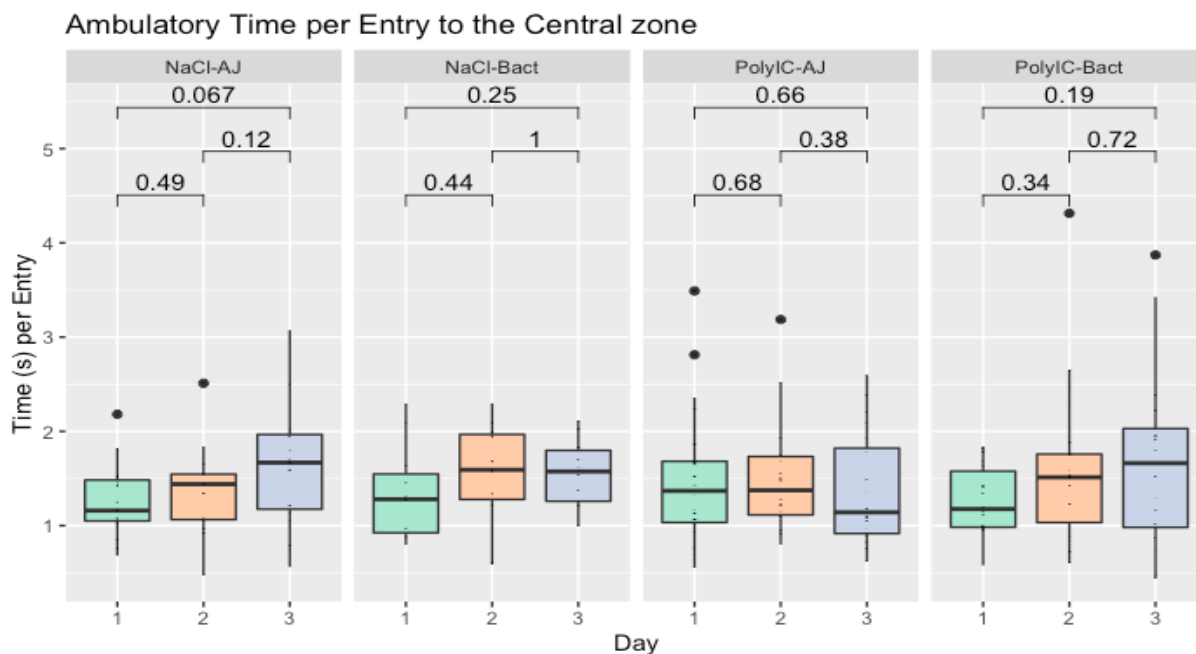


**Figure 10:** Time per entry in seconds in the center arena of the open field during the 3 days of habituation. NaCl = Sodium Chloride injected mouse, AJ= Apple Juice, Bact = amended with *Clostridium celatum*, PolyIC- PolyIC injected mouse;  $n = 10-20/\text{group}$

The reduction in locomotor or exploratory behavior after repeated exposures to the same environment has also been considered as a measure of habituation (Bolivar, 2009). So, we also measured the total distance traveled by mice in the open field. As indicated in Figure 11, NaCl-AJ mice showed a significant decrease in the distance traveled on Day 2 and Day 3, compared to Day 1 ( $p$  value  $<0.05$ , wilcox test), where the mice seem to habituate to the arena. Similar trend was also observed in PolyIC-AJ mice, which suggested that they also habituated on Day 2 and Day 3 when using this measure. Effect of *C. celatum* supplementation was seen in both NaCl and PolyIC mice as there was no significant change in the distance traveled by NaCl-Bact and PolyIC-Bact mice. A repeated ANOVA was also calculated and the effect of ‘Day’ ( $p$ -value= 0.049) and “Treatment” ( $p$ -value = 0.018) on the distance traveled in the center arena was found to be significant.

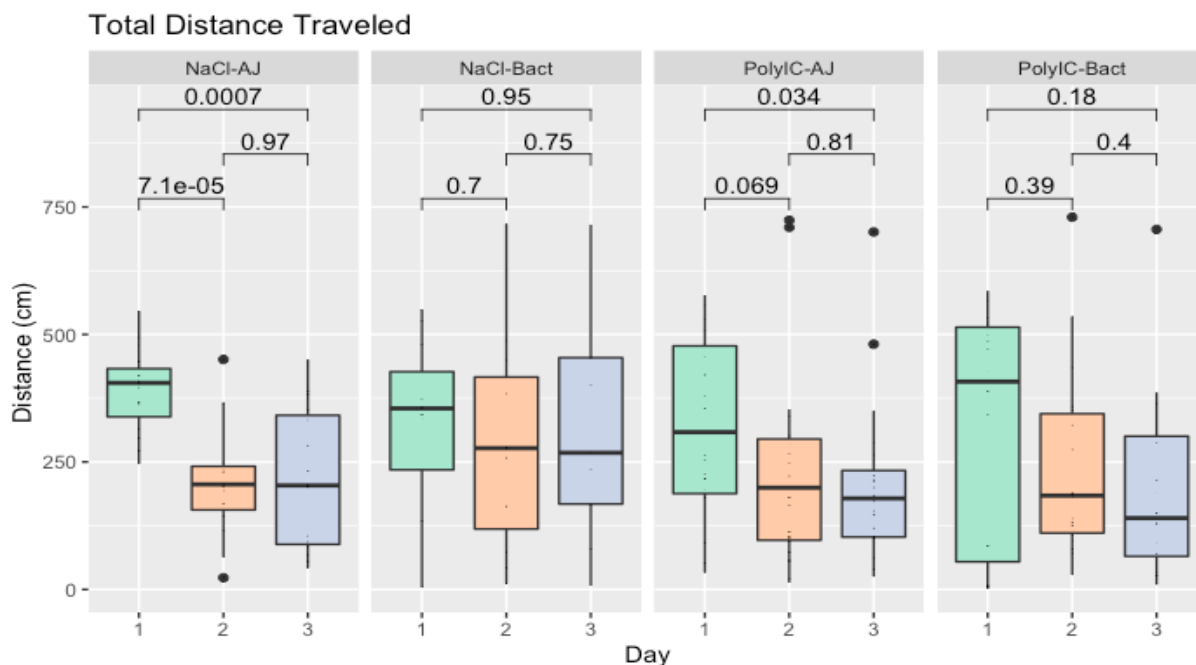


**Figure 11:** Total distance traveled in the open field during the 3 days of habituation. NaCl = Sodium Chloride injected mouse, AJ= Apple Juice, Bact = amended with *Clostridium celatum*, PolyIC- PolyIC injected mouse; n = 10-20/group

#### 4.1.4 Elevated Plus Maze

C57BL/6 mice who were fed either apple juice or apple juice containing *C. celatum* (Figure 5) for 4 weeks underwent the elevated plus maze test. For this test, mice were placed in the center of a plus-shaped maze consisting of two opposing open arms and two opposing closed arms. The test is based on the mice exploratory pattern, which avoids open and elevated spaces. The open space-induced anxiety of mice was determined by measuring the time spent in closed arms (Figure 12) and time spent in open arms (Figure 13). As we can see, there was no significant change in the time spent in either the closed arms or the open arms. The results were not significant after we performed ANOVA (p value > 0.05).

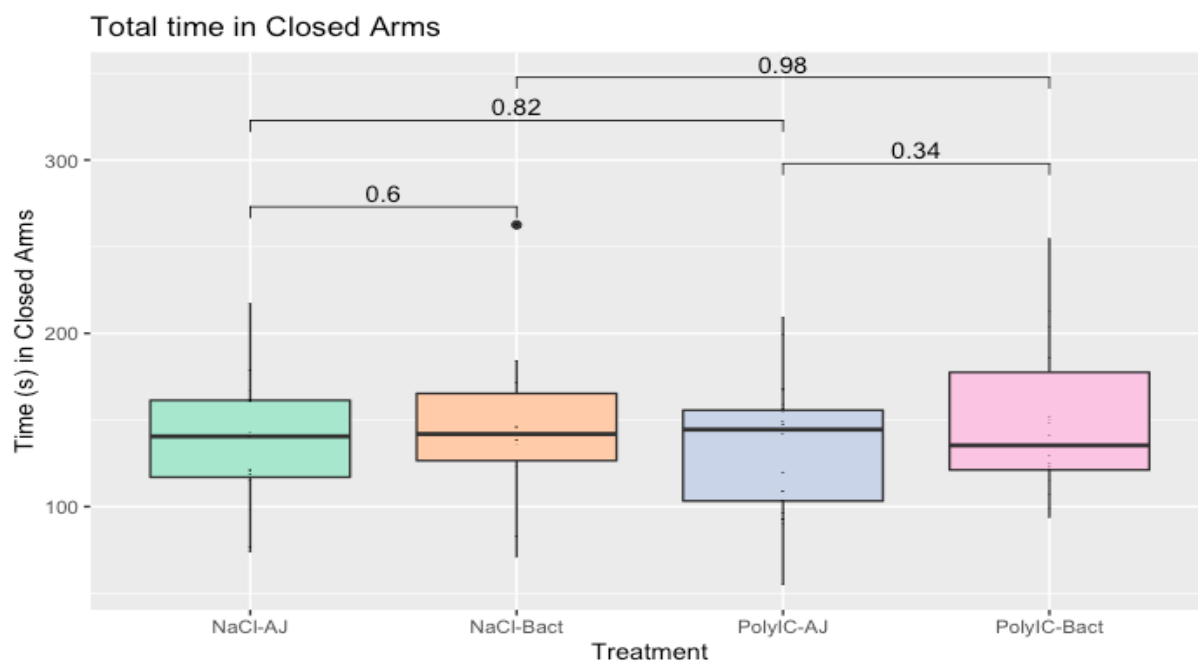


**Figure 12:** Time in seconds spent in the closed arms of the elevated plus maze. NaCl = Sodium Chloride injected mouse, AJ= Apple Juice, Bact = amended with *Clostridium celatum*, PolyIC- PolyIC injected mouse;  $n = 10-20/\text{group}$

We also observed the ratio of time spent in closed arms to total time spent in closed arms and open arms. As seen in Figure 14, the ratio of time spent in closed arms was not significant either ( $p \text{ value} > 0.05$ , wilcox test). The results were not significant using an ANOVA ( $p \text{ value} > 0.05$ ).

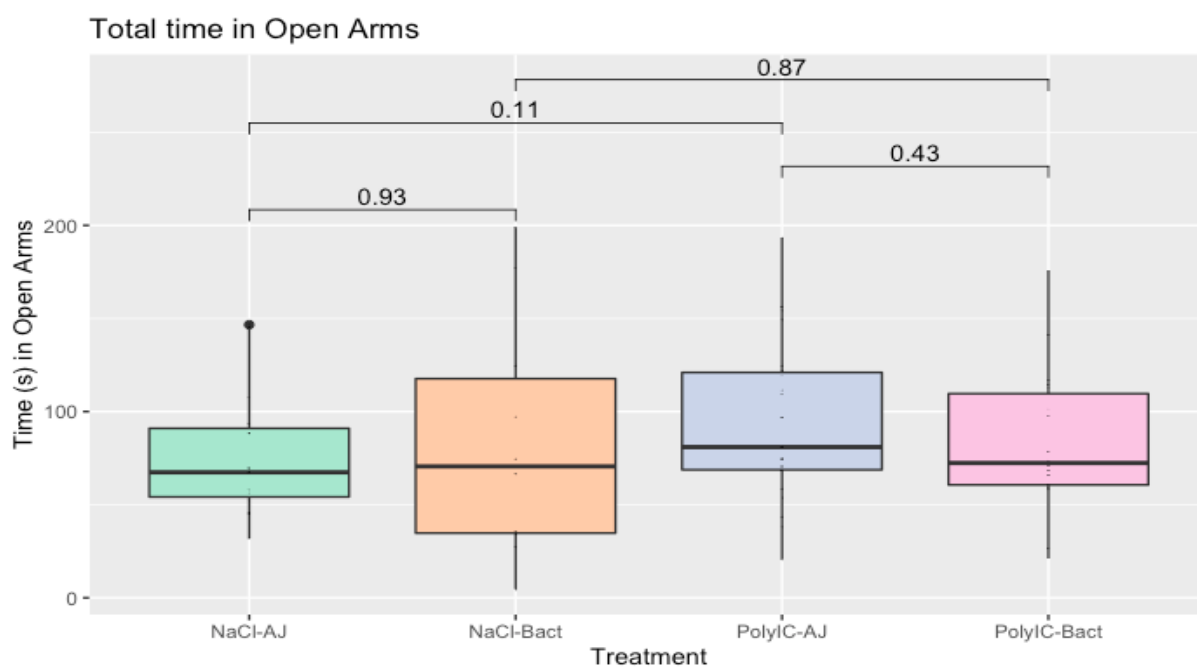


**Figure 13:** Time in seconds spent in the open arms of the elevated plus maze. NaCl = Sodium Chloride injected mouse, AJ= Apple Juice, Bact = amended with *Clostridium celatum*, PolyIC- PolyIC injected mouse;  $n = 10-20$ /group

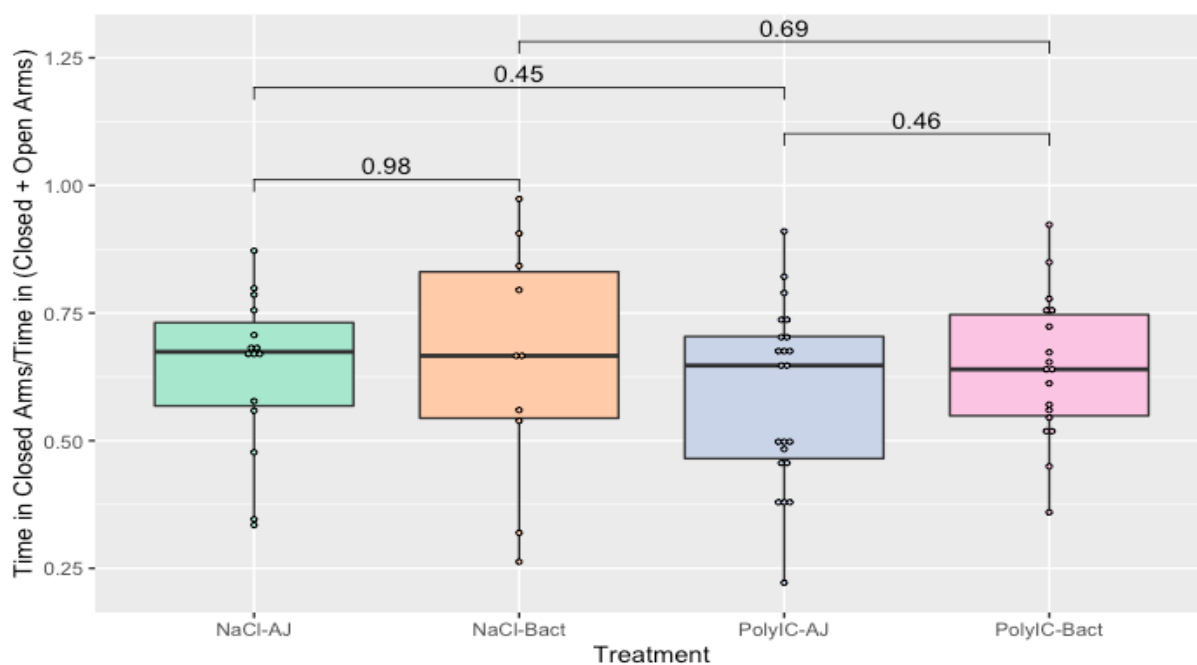


**Figure 14:** Ratio of time spent in open arms to total time spent in closed and open arms of the elevated plus maze. NaCl = Sodium Chloride injected mouse, AJ= Apple Juice, Bact = amended with *Clostridium celatum*, PolyIC- PolyIC injected mouse;  $n = 10-20$ /group

#### 4.1.5 Marble Burying

C57BL/6 mice were fed either apple juice or apple juice containing *C. celatum* (Figure 5) for 4 weeks and then marble burying test was performed. Marble burying measures repetitive and compulsive-like behaviors in mice. It uses the natural digging behavior of mice, which is aggravated if they are anxious. The number of marbles buried by different treatment groups of mice is demonstrated in Figure 15. Saline injected mice who were fed *C. celatum* in apple juice (NaCl-Bact) seemed to bury more marbles than NaCl-AJ mice, but the difference is not significant (p value = 0.95, wilcox test). PolyIC injected mice who were fed apple juice (PolyIC-AJ) buried marginally more number of marbles than NaCl-AJ group (p value = 0.1, wilcox test). There was no significant difference in the number of marbles buried by the PolyIC-AJ and PolyIC-Bact mice. The results were not significant using ANOVA (p value > 0.05).

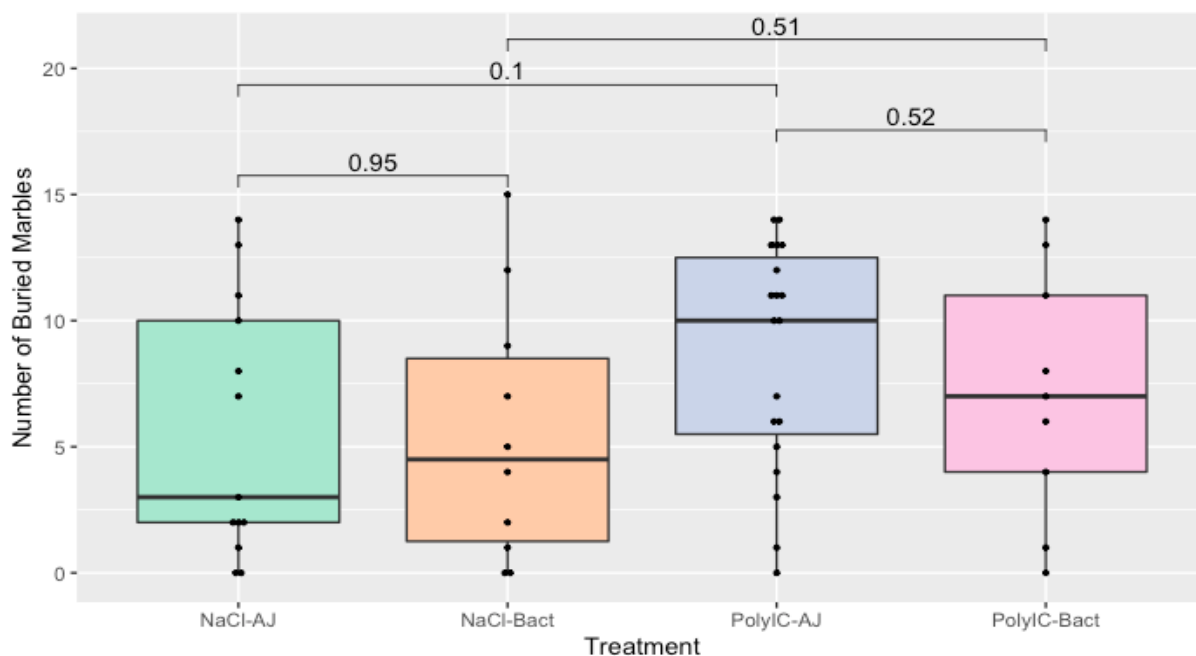
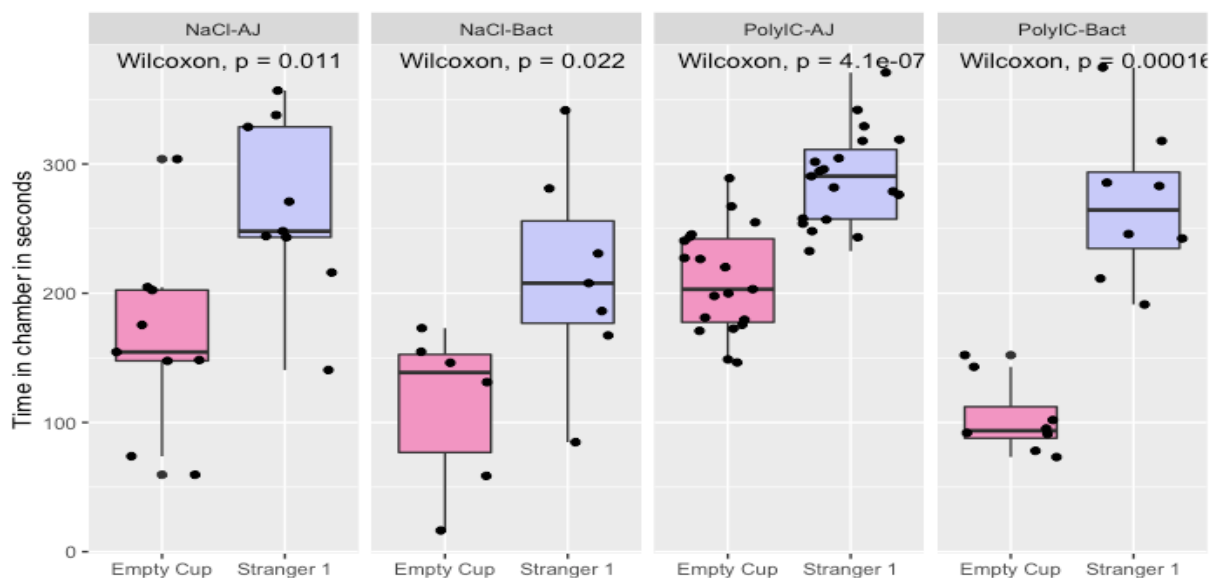


**Figure 15:** Number of marbles buried by the four treatment groups of mice. NaCl = Sodium Chloride injected mouse, AJ= Apple Juice, Bact = amended with *Clostridium celatum*, PolyIC- PolyIC injected mouse; n= 10-20/group

#### 4.1.6 Three Chambered Sociability and Social Novelty test

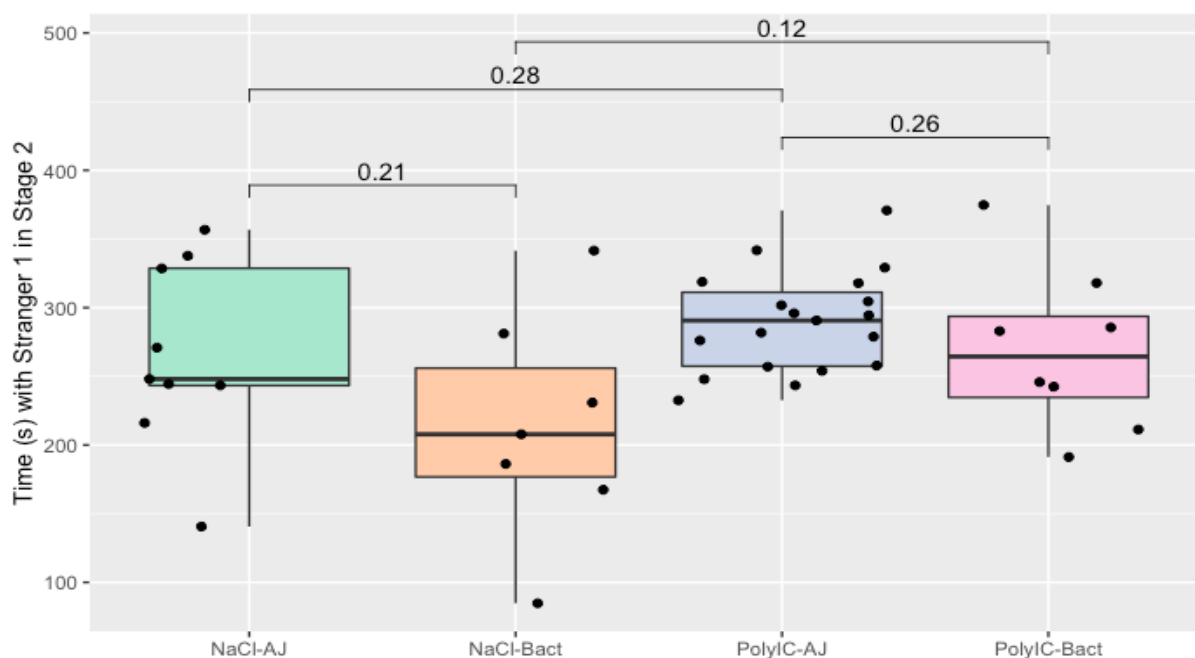
C57BL/6 mice were fed either apple juice or apple juice containing *C. celatum* (Figure 5) for 4 weeks and then this test was performed. After habituating the mouse for 5 minutes during stage 1, the testing mouse was given the opportunity during stage 2 to interact with a novel mouse (stranger 1) and a novel object (empty cup). Here, the mouse was tested for “sociability”, if it prefers to spend time with the novel mouse over the novel object (Lo et al., 2016). In the third and final stage, the testing mouse was placed in the center and was allowed to interact with stranger 1 (previously encountered) and stranger 2 (never-before-met mouse) to determine the “social novelty”.

Figure 16 compares time spent with the novel object and novel mouse during stage 2 of the test. Saline injected mice, when fed apple juice (NaCl-AJ), spent significantly more time with stranger 1 as compared to the empty cup (p value <0.05, wilcox test). The difference between time spent was reduced in the NaCl-Bact group. This difference was further reduced in the PolyIC injected group, who were fed apple juice (PolyIC-AJ). The difference in the time spent significantly increased in the PolyIC-Bact group (p value <0.05, wilcox test).



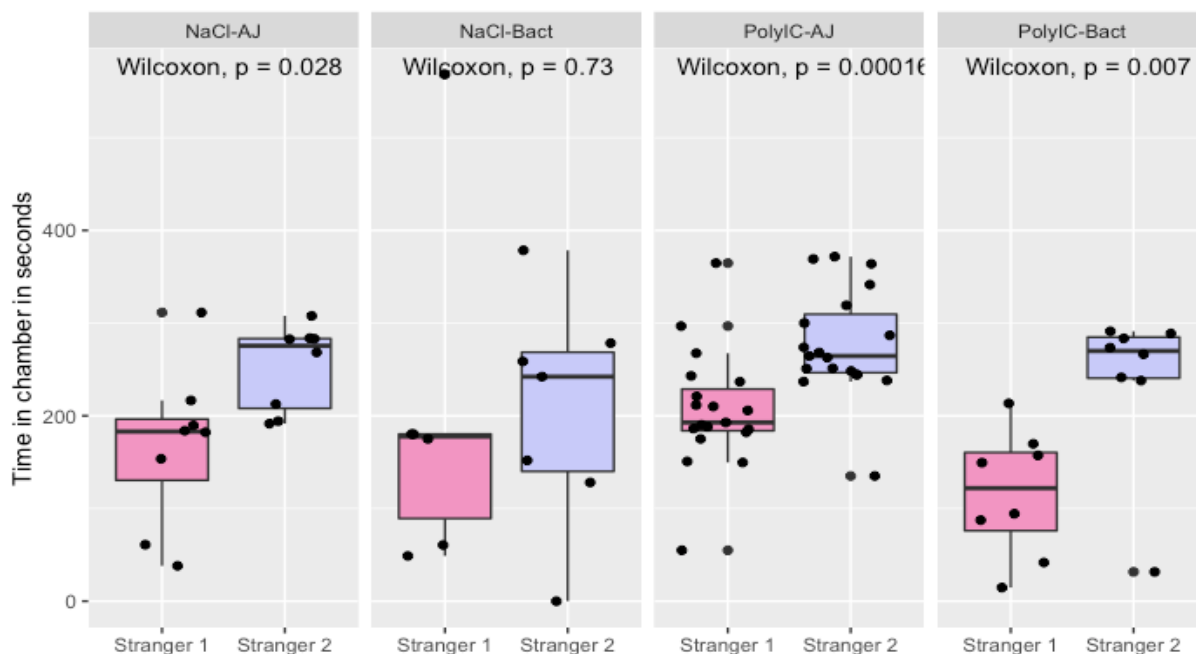
**Figure 16:** Time spent in seconds with empty cup (novel object) and stranger 1 (mouse) for all the treatment in the stage 2 of the test. NaCl = Sodium Chloride injected mouse, AJ = Apple Juice, Bact = amended with *Clostridium celatum*, PolyIC - PolyIC injected mouse;  $n = 8-18/\text{group}$ .

Figure 17 compares the time spent with the mouse during stage 2 of the test. Saline injected mice seemed to spend less time with stranger 1 when fed *C. celatum* in apple juice as compared to NaCl-AJ group, but the difference was not significant ( $p$  value = 0.21, wilcox test). PolyIC injected mice showed a similar trend but there was no significant difference in the time spent with stranger 1 between the two treatment groups ( $p$  value = 0.26, wilcox test). This was neither significant using an ANOVA.



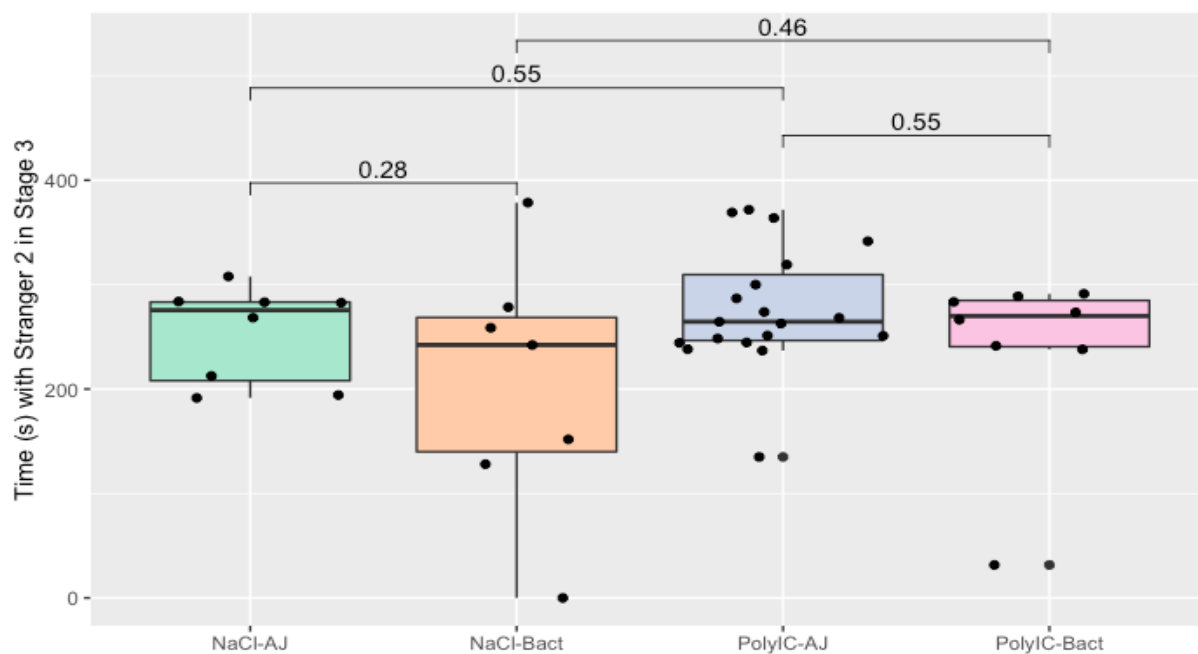
**Figure 17:** Time spent in seconds with Stranger 1 (mouse) across all the treatments in the stage 2 of the test. NaCl = Sodium Chloride injected mouse, AJ= Apple Juice, Bact = amended with *Clostridium celatum*, PolyIC- PolyIC injected mouse;  $n=8-18/\text{group}$ .

Figure 18 compares time spent with the stranger 1 (previously encountered) and stranger 2 (never-before-met) during the final stage of the test. Saline injected mice, when fed apple juice (NaCl-AJ), spent significantly more time with stranger 2 as compared to the stranger 1 ( $p$  value  $<0.05$ , wilcox test). This significance was lost in NaCl-Bact group ( $p$  value = 0.7, wilcox test). The difference between time spent with stranger 1 and stranger 2 in the PolyIC injected group was not affected by *C. celatum*, as both groups spent significantly more time with stranger 2 than stranger 1 (Figure 18).



**Figure 18:** Time spent in seconds with stranger 1 and stranger 2 during the final stage of the test, compared for all the treatment groups of mice. NaCl = Sodium Chloride injected mouse, AJ= Apple Juice, Bact = amended with *Clostridium celatum*, PolyIC- PolyIC injected mouse  $n = 8-18/\text{group}$ .

The time spent with stranger 2 during stage 2 is seen in Figure 19. Saline injected mice spent less time with stranger 2 when fed *C. celatum* in apple juice as compared to NaCl-AJ group, but the difference was not significant ( $p$  value  $>0.05$ , wilcox test). PolyIC injected mice showed a similar trend but there was no significant difference in the time spent with stranger 2 between the two treatment groups. The difference was not significant for any of the groups using an ANOVA ( $p$  value  $>0.05$ ).



**Figure 19:** Time spent in seconds with stranger 2 in the final stage of the test. NaCl = Sodium Chloride injected mouse, AJ= Apple Juice, Bact = amended with *Clostridium celatum*, PolyIC- PolyIC injected mouse  $n= 8-18/\text{group}$ .

## 4.2 Enteroendocrine cells (EEC), vagal nerve and the gut microbiome

Recent studies have shed light on EEC sensory transmission by showing direct connections between EECs and the nervous system via axon-like processes known as neuropods, through which EECs can directly communicate with the neurons innervating the GI tract (Latorre et al., 2016). We hypothesized that *C. celatum* and the other taxa in gut microbiota can potentially send signals to the brain via direct interactions with EECs. For this, we first cultured EECs by dissociating CCK-GFP mice intestine and isolating them from the other gut epithelial cells and then cross-linked them with the gut microbiota.

### 4.2.1 EECs viability after dissociation

Cell viability was determined using Trypan Blue assay. After counting total number of cells and blue/dead cells (Figure 20), cell viability was calculated as:

Cell viability =  $[1.00 - (\text{Number of blue cells} \div \text{Number of total cells})] \times 100$

Cell viability was mostly maintained at 85-87% before sorting to isolate EECs

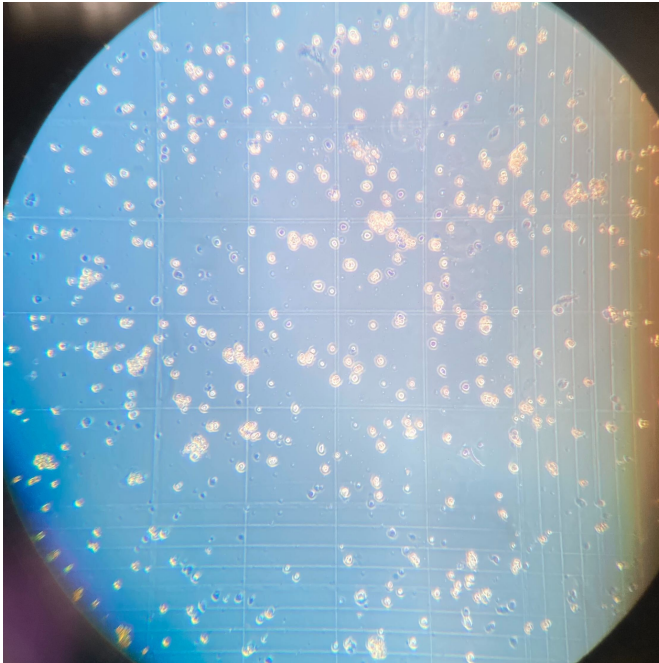


**Figure 20:** Gut epithelial cells after dissociation, stained with trypan blue, to measure cell viability by loading the hemocytometer. Dead cells are stained blue and viable/live cells are bright/unstained cells.

#### 4.2.2 Magnetic sorting of EECs

We attempted to magnetically sort EECs by using an antibody against Claudin-4 protein, which has been reported by researchers as a cell surface marker on EECs (Nagatake et al., 2014). All the cells were labeled with Phycoerythrin (PE)-conjugated anti-claudin-4 antibody and anti-PE microbeads were used to magnetically isolate them.

Figure 21 depicts the gut epithelial cells that were collected first, since they were not labeled and passed through the column. As we can see in GFP settings, GFP cells also passed through the column. Figure 22 shows the labeled cells and as can be seen, other epithelial cells (non-GFP) were also collected along with a very few GFP-EECs.

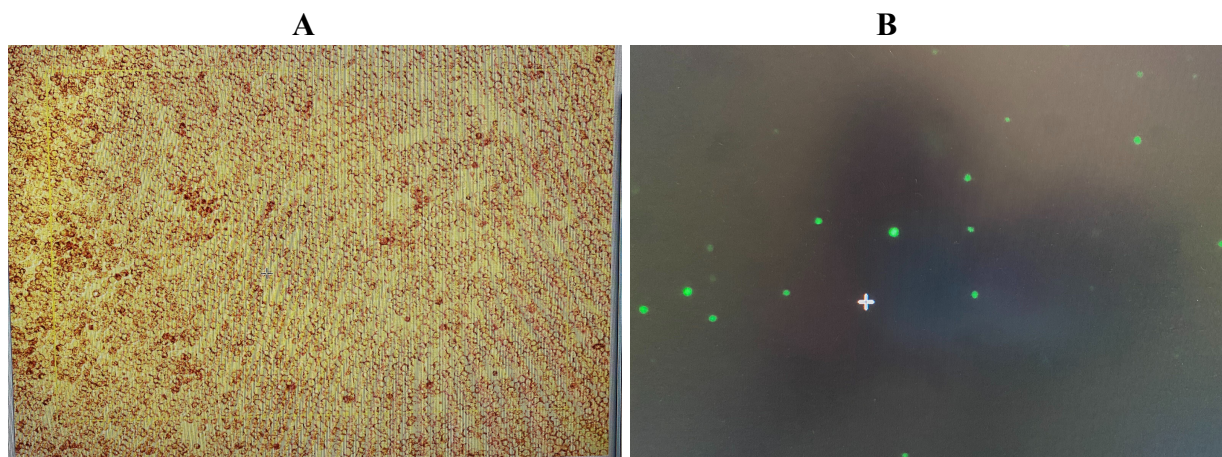


**Figure 21:** Unlabeled cells that passed through the column. A. Cells visualised under bright-field B. Cells visualised with GFP settings

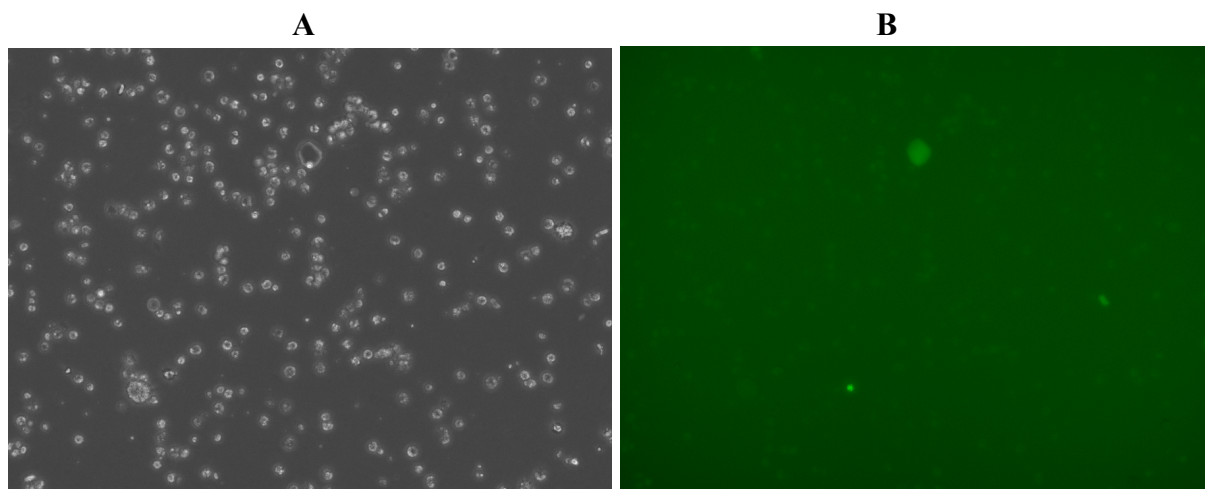


**Figure 22:** Labeled cells retained in the column and collected by flushing the column with a separation buffer. A. Cells visualised under bright-field B. Cells visualised with GFP settings

Since the labeling of EECs by PE-conjugated anti-claudin-4 antibody was not specific, as evident in Figure 21 and Figure 22, we performed flow cytometry analysis to check the expression of claudin-4 protein on all the gut epithelial cells. Figure 23 is the fluorescence plot generated by flow cytometer, and we can see that very few cells that are GFP labelled also express red fluorescence provided by Phycoerythrin (PE) fluorophore on the antibody (very few cells are on the top right quadrant of the figure). The analysis was performed multiple times, and the same results were observed.

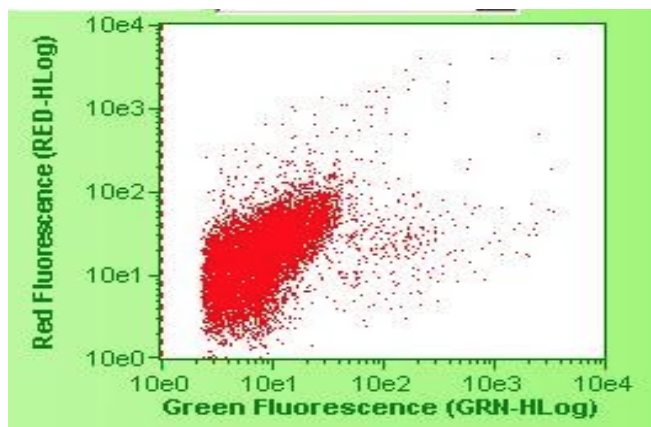


**Figure 23:** Flow cytometry analysis of the gut epithelial cells labeled with PE-conjugated Anti-Cld-4 antibody.

#### 4.2.3 EECs sorted by FACS and cultured overnight

We successfully sorted GFP-labeled EECs by Fluorescent Activated Cell sorting (FACS) and cultured them on matrigel coated 35 mm dishes at 37C (5% CO<sub>2</sub>). Figure 24 depicts the cells visualised under fluorescent microscope after an overnight incubation.

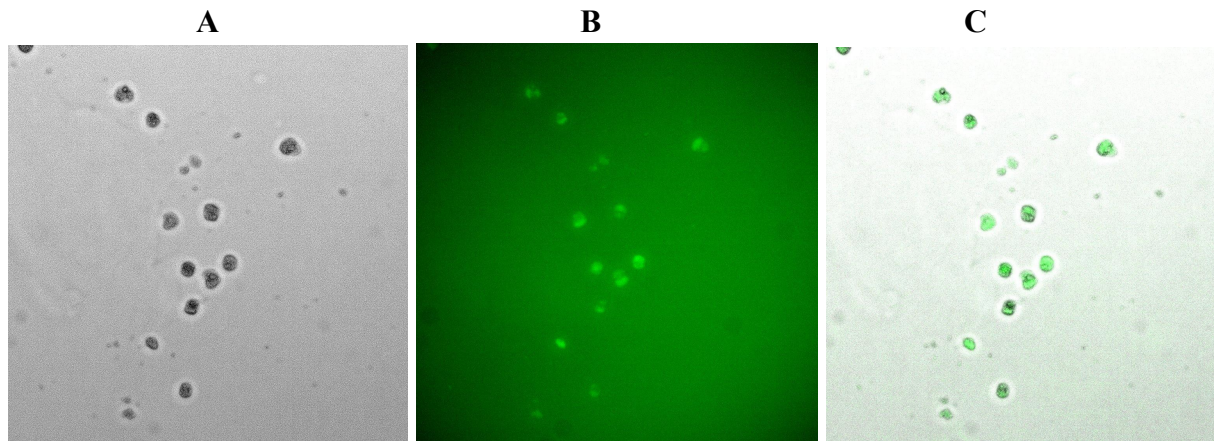


**Figure 24:** Entero-endocrine cells visualised under epifluorescent microscope after an overnight incubation. A. Bright-field image B. Green Fluorescent image C. Overlaid picture

#### 4.2.4 EECs-neurons co-culturing

We optimized the recapitulation of connection between EECs and vagus nerve by co-culturing them. The neurons extended their neurites, including towards GFP-labeled EECs, (Figure 25).

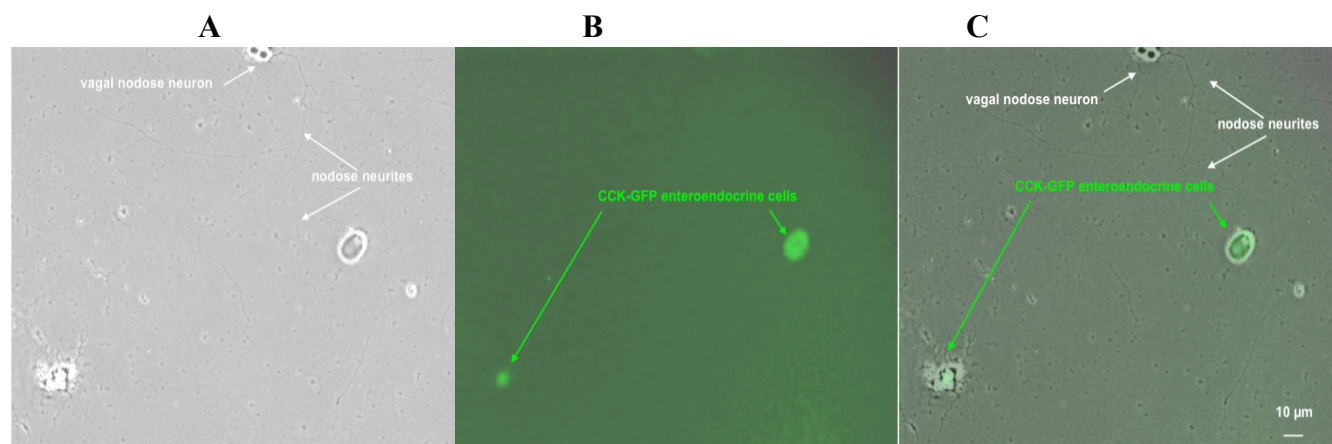


**Figure 25:** Co-culture of vagal nodose neurons and EECs. *A.* Nodose neurons visualised under bright-field *B.* EECs visualized with GFP settings *C.* Overlaid picture showing both vagal nodose neurons and GFP-labeled EECs

#### 4.2.5 EECs-gut microbiota crosslinking

In order to determine if the gut microbiota can directly interact with EECs to transduce signals to the brain via vagus nerve, we covalently crosslinked gut microbiota with EECs. Samples with amendment ‘Bacterial Wash (BW)’ contain non-interacting bacteria that didn’t crosslink with EECs, and samples with ‘Cross Link (Xlink)’ amendment contain crosslinked EECs and gut bacteria. PCoA plots in Figure 26 show the clear distinction between EEC-Bacterial Wash and EEC-Cross link samples when constrained by amendment.

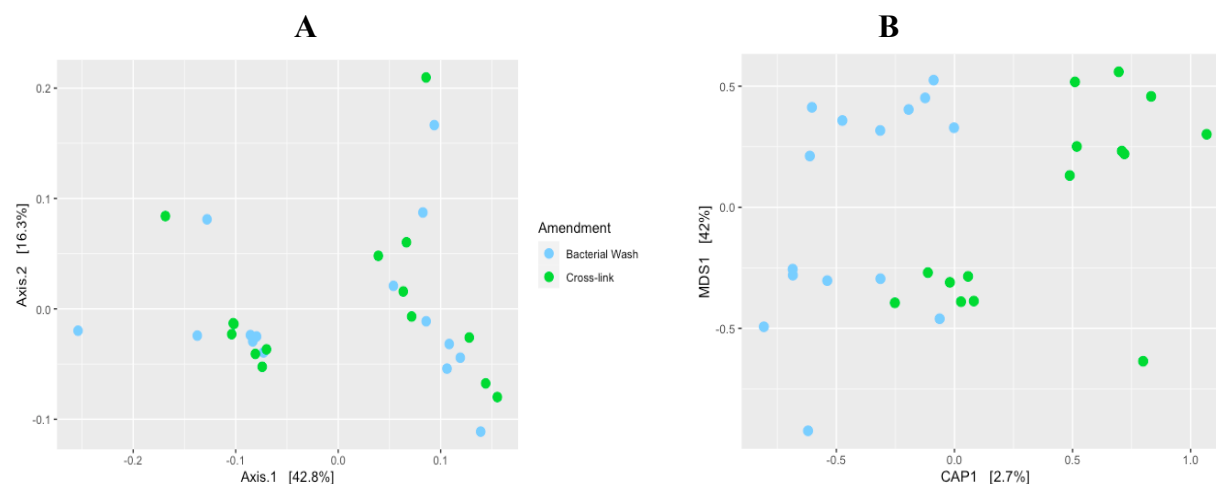


**Figure 26:** Principal Coordinate analysis (PCoA) plot of Bray- Curtis distances between all EEC-Bacterial Wash and EEC-cross linked samples, *A.* Unconstrained *B.* Constrained by Amendment

We compared the sequencing depth of all three types of samples (Figure 27) to confirm that there was no significant difference in the read depth of the three samples (p-value < 0.15, Wilcox test).

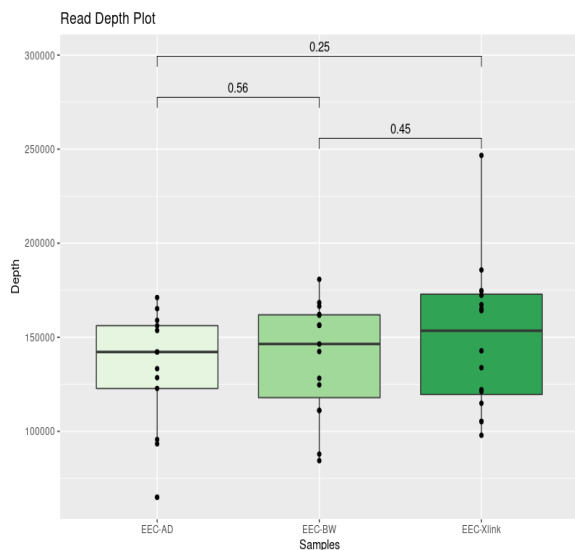


**Figure 27:** Comparable sequencing depth of EEC-AD, EEC- BW and EEC-cross linked samples, dots are samples

Next, we plotted the relative abundance of all the genus found in the top 50 most abundant ASVs in EEC-BW and EEC-Crosslink samples (Figure 28).

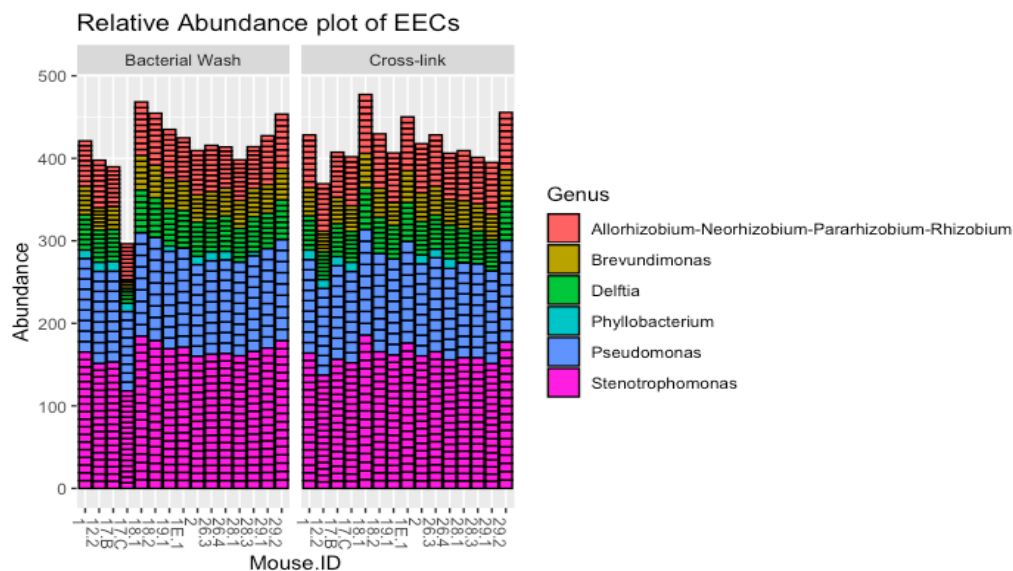


**Figure 28:** Relative abundance of taxa found in top 50 most abundant ASVs in EEC- BW and EEC- cross linked samples at the genus level

Significantly different ASVs in the two amendments: EEC-BW and EEC-Xlink were determined by performing a Wilcox test on all the ASVs present. As can be seen in Figure 29, ASV65, ASV69, ASV72, ASV74, ASV80, and ASV81 are the ASVs that were found to be significantly more abundant in ‘EEC-crosslink’ amendment as compared to the ‘EEC- BW’ amendment and when annotated at the family level, all the significant ASVs belonged to the *Rhizobiaceae* family. We also plotted a phylogenetic tree of the *Rhizobiaceae* family with the ASVs as tip labels and as we can see in Figure 30, they all belonged to one clade and were placed next to each other.

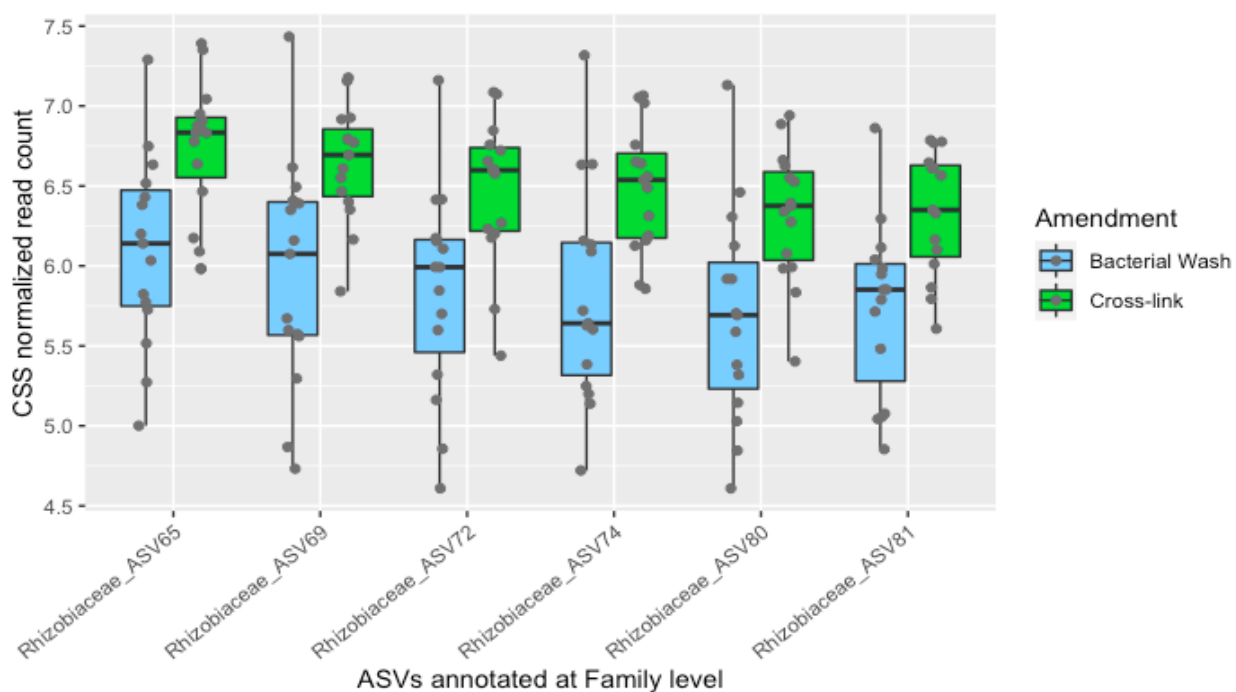


**Figure 29:** FDR corrected Wilcox test. Abundance plot of significant different ASVs (annotated at Family level) in EEC- BW and EEC- Cross-link Amendment (FDR adjusted p value <0.15, wilcox test)

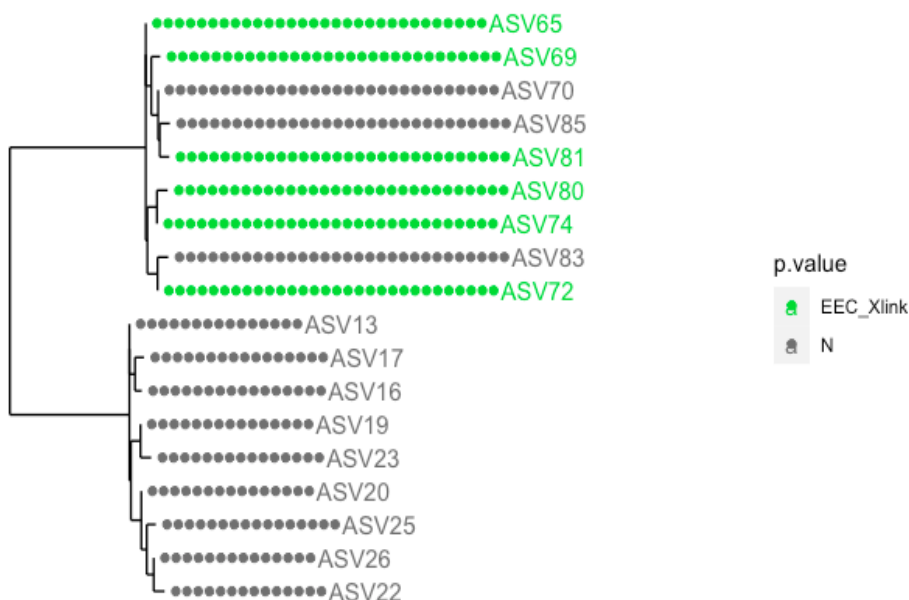


**Figure 30:** Phylogenetic tree of family *Rhizobiaceae* showing significant different ASVs (Wilcox test) in EEC-Xlink amendment in green and the non-significant ASVs in gray.

We also performed an ANCOM test to find the significantly different ASVs in the two amendments: EEC-BW and EEC-Cross-link. Results were pretty similar to that of the Wilcox test. The ASVs that were significantly more abundant in the EEC-cross link amendment included ASV65, ASV69, ASV70, ASV72, ASV74, ASV80, ASV81, ASV83, and ASV85 which belong to the *Rhizobiaceae* family, and ASV55 and ASV58 from the *Lactobacillaceae* family. Two ASVs were found that were significantly more abundant in EEC-BW: ASV235 from the *Halomonadaceae* family and ASV258 from the *Pseudomonadaceae* family (see Figure 31). These ASVs are classified at all the levels in Table 2.

These significant ASVs and the non-significant ASVs from the *Rhizobiaceae* family were also observed on a phylogenetic tree and as it can be observed in Figure 32, all the significant ASVs (green colored) belonged to one clade, lied next to each other and the non-significant ASVs (gray colored) belonged to the other clade.

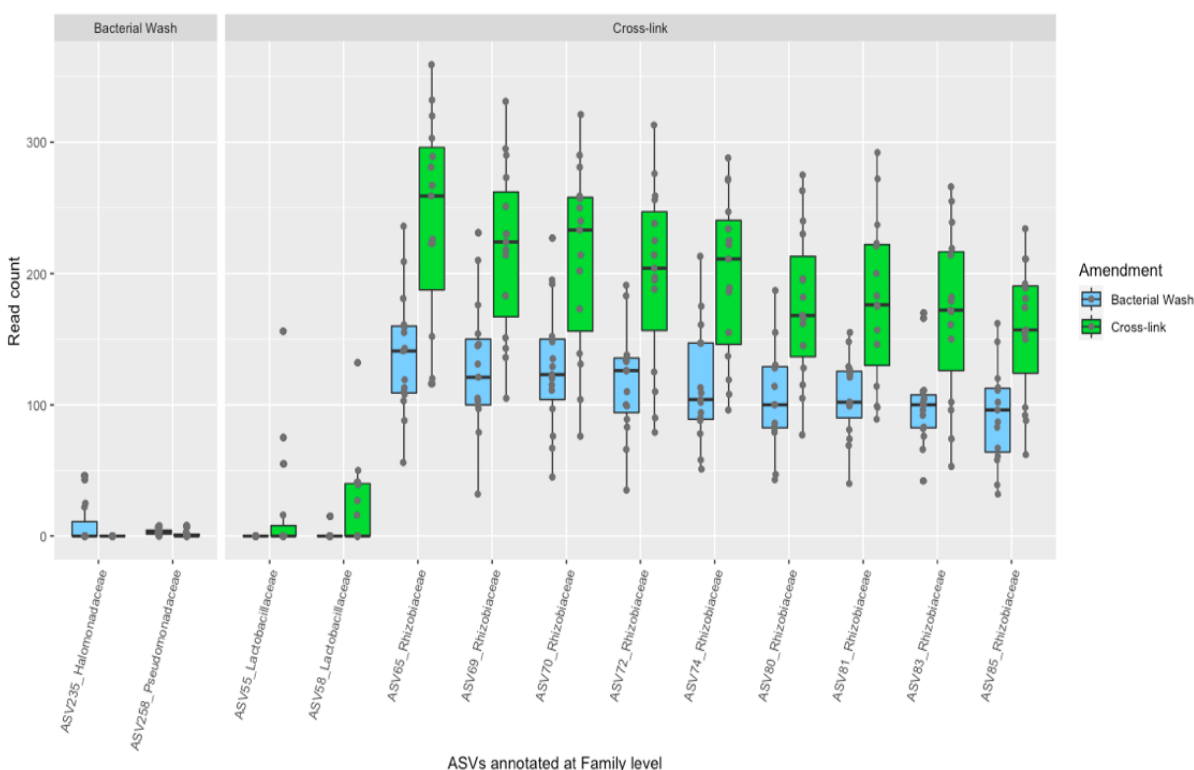


**Figure 31:** ANCOM test. Abundance plot of significant different ASVs (annotated at Family level) in EEC- BW and EEC- Cross-link Amendment ( $p$  value  $< 0.15$ , ANCOM test)

**Table 6:** Significant ASVs in EEC-BW and EEC-cross-link samples, classified at the phylum, order, family and genus level.

ASVs more abundant in BW				
ASV	Phylum	Order	Family	Genus
ASV235	Proteobacteria	Oceanospirillales	Halomonadaceae	Halomonas
ASV258	Proteobacteria	Pseudomonadales	Pseudomonadaceae	Pseudomonas
ASVs more abundant in EEC X-linked				
ASV	Phylum	Order	Family	Genus
ASV55 ASV58	Firmicutes	Lactobacillales	Lactobacillaceae	Lactobacillus
ASV65 ASV69 ASV70 ASV72 ASV74 ASV80 ASV81 ASV83 ASV85	Proteobacteria	Rhizobiales	Rhizobiaceae	Allorhizobium- Neorhizobium- Pararhizobium- Rhizobium

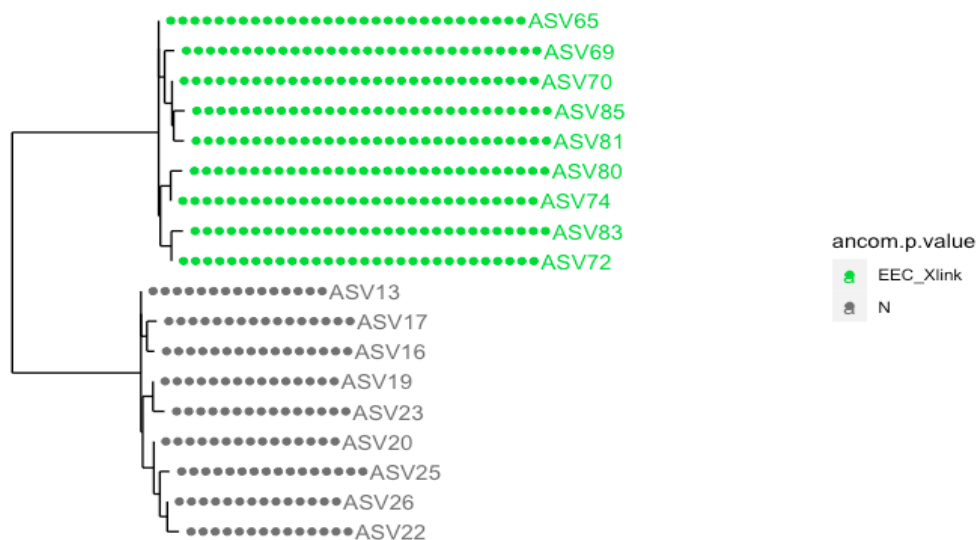


**Figure 32:** Phylogenetic tree of family Rhizobiaceae showing significant different ASVs (ANCOM test) in EEC-Xlink amendment in green and the non-significant ASVs in gray color.

Same analyses were also performed for the negative cells. Negative cells are all the other gut epithelial cells (non-GFP EECs). The Wilcox test found no significant ASV and the ASVs that were found to be significantly different by the ANCOM test (Figure 33) were completely different from the significant ASVs in the EEC cell population.

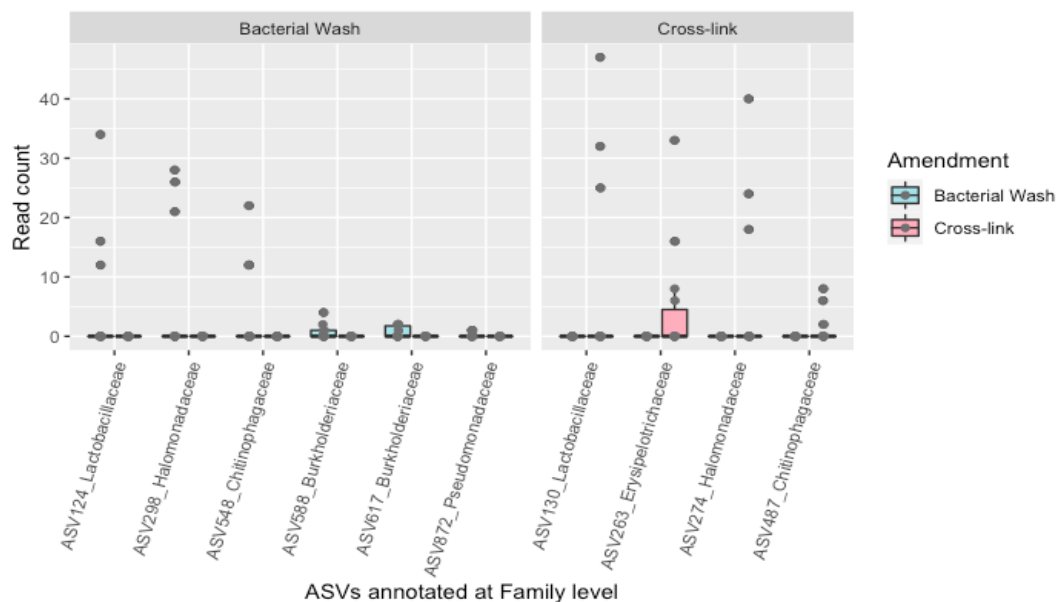


**Figure 33:** Abundance plot of significant different ASVs (annotated at Family level) in Neg- BW and Neg- Cross-link Amendment ( $p$  value  $< 0.15$ , ANCOM test)

Plotting the significant ASVs from the *Lactobacillaceae* family in EECs and negative cell population on the phylogenetic tree (Figure 34) showed a clear separation of the ASVs. The ASVs in EECs and negative cells belonged to different clades and lied far away from each other.

Plotting the significant ASVs from the *Lactobacillaceae* family in EECs and negative cells on the phylogenetic tree (Figure 34) shows a clear separation of the ASVs. ASV55 and ASV 58, which are found to be significantly more abundant in EEC-cross linked amendment belong to one clade. ASV124 which was found to be significantly more abundant in negative cells-bacterial wash and ASV130, which was found to be significantly more abundant in negative-cross link amendment belong to the other clade and they are very far away from each other.

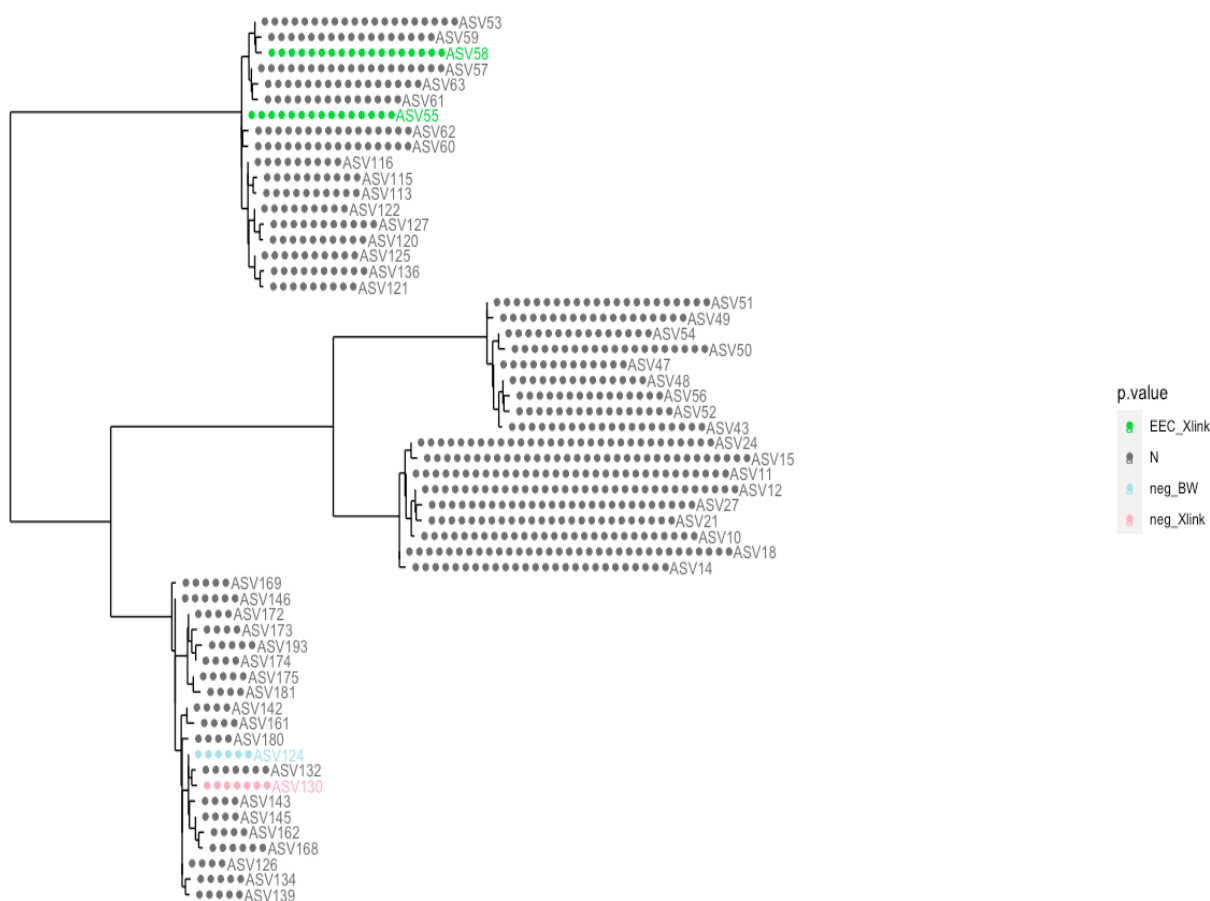


**Figure 34:** Phylogenetic tree of family *Lactobacillaceae* showing significant different ASVs in EEC-Xlink amendment in green, in Neg-Xlink amendment as pink, in Neg-BW amendment as blue, and the non-significant ASVs in gray.

#### 4.2.6 EECs- *C. celatum* crosslinking

EECs were also cross-linked with anaerobically grown *C. celatum* mixed with the other gut microbiota to see if *C. celatum* can interact with EECs. First, by performing 16S BLAST on all the ASVs in the ‘*C. celatum* and gut’ samples against *C. celatum* DSM 1785 16S rRNA gene, we found 8 ASVs closest to *C. celatum* (>90% similarity BLAST). Figure 35A shows the ASV798 and ASV906 which were found to be significantly abundant in the ‘*C. celatum* and gut’ EEC-crosslinked samples. These two ASVs were not present in the positive control (*C. celatum* only) (Figure 35B).

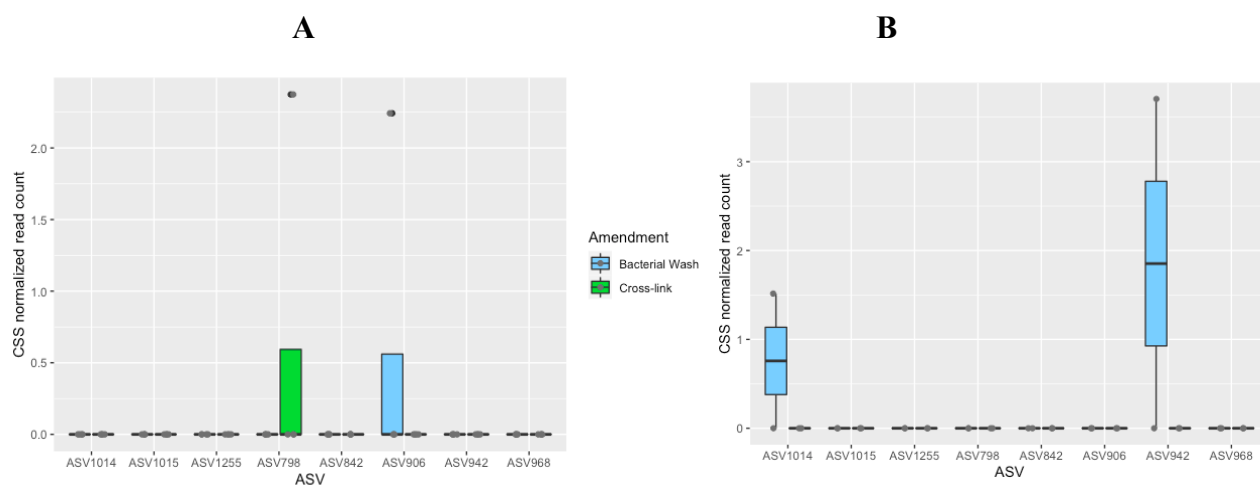


**Figure 35:** Abundance of ASVs similar to *C. celatum* (>90% similarity) in A. Gut sample spiked with *C. celatum*. B. *C. celatum* samples (positive control)

## 5. Discussion

### 5.1 *C. celatum* in the gut- brain axis

The gut-brain axis refers to the bidirectional communication that takes place between the brain and GI tract, linking emotional and cognitive centers of the brain with peripheral intestinal mechanisms such as intestinal permeability, immune activation and entero-endocrine signaling (Breit et al., 2018; Carabotti et al., 2015). Many studies have associated the gut microbiota with the brain function (Martin et al., 2018). While the beneficial effects of gut microbiota on behavior have been well studied (Messaoudi et al., 2011), less is known about the negative impacts of gut microbiota on the behavioral phenotypes. In this study, we supplemented the gut microbiota of the C57BL/6 mice with *Clostridium celatum*, which was found to be elevated in children with ASD (David et al., 2018). We fed the bacteria in apple juice 3 times a week to maintain a constant colonization of the bacteria in the mice gut.

We first tested the viability of *C. celatum* in apple juice at different time intervals (Table 5) and found that 2000 CFU/ml was still found after 48 hours, which allowed us to conclude that the bacterial cells were still alive within the 2 h window during which the mice eat the apple juice. This result supports our feeding design, which allowed to supplement the mice with *C. celatum* without gavaging them, and subsequently avoid stress that could be reflected in the behavior tests. However, we didn't plate the original number of bacteria in the media, so we do not have an estimate of the number of bacteria that were affected by transiting in the apple juice (as 2000 CFU seemed very low). We also noted important discrepancy in the different dilutions during our plating, possibility of underestimation of CFU/ml, which would require us to replicate this experiment. Several behavioral assays including a) Open field habituation test b) Elevated plus maze test c) Marble burying test d) Three chambered sociability and social novelty test, were performed to determine the impact of *C. celatum* on mice anxiogenic phenotypes.

*C. celatum* supplementation affected the habituation in our control mice (saline injected) since there was no significant increase in the time spent in the center per entry by *C. celatum* fed mice (NaCl- Bact) mice, after repeated exposure to the same environment (Figure 10). This

seemed to indicate that non ASD-model mice were affected by the addition of *C. celatum*. Our autism mouse models (PolyIC-injected mice)(Malkova et al., 2012) didn't habituate either on Day 2 and Day 3, which is consistent with the literature (Hsiao & Patterson, 2011).

In the same test, we observed that the distance traveled by the control mice decreases with each passing day due to the reduction in locomotor or exploratory behavior after repeated exposures (Hefner & Holmes, 2007; Bolivar, 2009; Bothe et al., 2004). Accordingly, we observed that NaCl-AJ and PolyIC-AJ mice showed a significant decrease in the distance traveled on Day 2 and Day 3. The effect of *C. celatum* was seen in both NaCl and PolyIC mice as there was no significant change in the distance traveled by NaCl-Bact and PolyIC-Bact mice after repeated exposures (Figure 11). Such behavior results seem to pinpoint possible anxiogenic or negative impacts on non-associative learning by *C. celatum* on both mice models. On the other hand, the elevated plus maze test, which also measures the anxiety of mice by measuring the time spent in closed arms, didn't provide any significant results (Figure 12, Figure 13 and Figure 14).

The marble burying test provided some results correlating the habituation results: PolyIC-AJ mice buried more marbles than NaCl-AJ mice (Figure 15). However, no effect of *C. celatum* on the number of marbles buried was observed, which suggests that *C. celatum* doesn't affect the repetitive digging behavior of mice.

The three chambered sociability and social novelty test assesses the social behavior of mice. *Sociability* is defined as the propensity of the mouse to spend time with a novel mouse as compared to a novel object and *social novelty* is defined as the propensity of mouse to spend more time with an unfamiliar mouse as compared to a familiar one (Kaidanovich-Beilin et al., 2011). As we can see in Figure 16, all four groups of mice spent significantly more time with the novel mouse as compared to the novel object. The difference in the time spent was reduced in NaCl-Bact mice, which suggests the negative effect of *C. celatum* on *sociability* of the mice. PolyIC-AJ mice also exhibited similar sociability. And the effect of *C. celatum* on sociability was not seen in PolyIC, indicating possible issues with the test as the literature indicates a clear difference between the two models for this test. The data would need to be better explored, we

have not for example considered the time spent in the middle, and could work with percentage instead of raw time spent in each zone. It is difficult to draw any conclusion here given the lack of consistency of the results in our control groups: the team needs to take in account the time in the center and/or increase the sample size. Given that the PolyIC phenotype is clearly observed in the other test, we do not believe that the injection of PolyIC is the issue here.

## **5.2 Enteroendocrine cells, vagal nerve, and the gut microbiome**

The focus of the second part of this study was to determine the mechanism by which the gut microbiota modulates the behavior in mice. Recently, researchers identified a type of gut sensory cells that synapses with vagal neurons, designated as enteroendocrine cells (EECs). As demonstrated in Figure 1, open-type EECs which are also regarded as *chemosensors* can sense the luminal contents and release secretory products in basal lamina, where they can act locally or enter systemic circulation (Sternini et al., 2008). It has also been established that EECs can sense glucose and transduce the signals to the brain via the vagus nerve (Kaelberer et al., 2018). But there is a lack of knowledge in understanding if the gut microbiota can directly interact with these EECs. To understand if *C. celatum* and other taxa in the gut microbiome modulate brain activity through direct interaction with EECs, we optimized isolation of EECs and their connection with vagal neurons. Next, we covalently cross-linked EECs with *C. celatum* and the other taxa in the gut microbiota using Sulfo-SBED.

### *5.2.1 Optimization of isolation of EECs*

After dissociation of the small intestine of CCK-GFP mice, cells were visualised under microscope to determine cell viability, which was found to be around 85%. Cells appeared bright and viable (Figure 20), but to confirm its functionality, electrophysiology is recommended. Isolation of EECs from the other intestinal epithelial cells is a very challenging process as EECs represent only 1% of the intestinal epithelial cell population and they are always found isolated from one another, interspersed with other epithelial cells like paneth cells, goblet cells, and mucus cells (May & Kaestner, 2010); (Nagatake et al., 2014). The development of transgenic mice CCK- green fluorescent protein (GFP) has made their isolation relatively easier (Chandra et al., 2010). We tried several methods to isolate EECs, including magnetic sorting by using an

antibody against Claudin-4 protein, which has been reported by researchers to be present on the entire population of EECs (Nagatake et al., 2014). **But our flow cytometry results (Figure 23) demonstrated that not all the GFP-EECs were labeled with the antibody against the claudin-4 protein and other gut epithelial cells were also labeled with claudin-4 antibody .** These results should be taken into account when considering to isolate the EECs by using Claudin-4 as a cell surface marker for EECs. Finally, by fluorescence activated cell sorting (FACS), we were able to isolate GFP-labeled EECs, as we can see in Figure 26.

EECs are shown to have neuropods and a synaptic connection between the EECs and neurons have been proven using monosynaptic rabies virus (Bohórquez et al., 2015). We also optimized the recapitulation of connection between EECs and vagus nerve by co-culturing them (Kaelberer et al., 2018). As depicted in Figure 25, the neurons extend their neurites on the dish, including towards EECs. But to confirm if there is a synaptic connection between the EEC and the neurons we would need to do electrophysiology recordings.

### 5.2.2 Crosslinking of gut microbiota with EECs

We crosslinked the sorted EECs with the gut microbiota extracted from the intestine of the same CCK-GFP mouse, using a covalent cross-linking strategy with Sulfo-SBED. We generated three different kinds of samples described in Table 4. After Dilution (AD) samples contained the diluted bacteria that was used for crosslinking with EECs, Bacterial Wash (BW) samples had non interacting bacteria that didn't crosslink with EECs and Cross-link (Xlink) samples contained crosslinked EECs and gut bacteria. We called these three different kinds of samples as 'amendments' for 16S analysis. We also generated the same samples from negative cells. Negative cells are all the other gut epithelial cells (non-GFP EECs).

EECs were cross-linked with the gut microbiota from the same mouse, spiked with *C. celatum* to see if *C. celatum* can interact with EECs. Figure 35 shows that the ASVs that were found to be significantly abundant in '*C. celatum* and gut' EEC-crosslinked samples were not present in only *C. celatum* samples, suggesting that *C. celatum* didn't interact (cross-link) with EECs or that we could not detect it in the spiked samples.

To see if there are any other specific bacteria that could interact with EECs, we analysed the samples where EECs were crosslinked with all the gut microbiota from the same mouse. PCoA plots in Figure 26 show the clear distinction between EEC-Bacterial Wash and EEC-Cross link samples, when constrained by amendment. We performed a Wilcox test on all the ASVs present in these two amendments to find the significantly different ASVs. As can be seen in Figure 29 and Figure 30, ASV65, ASV69, ASV72, ASV74, ASV80 and ASV81 are the ASVs that were found to be significantly more abundant in ‘EEC-crosslink’ amendment as compared to the ‘EEC- BW’ amendment and when annotated at family level, all the significant ASVs belonged to the *Rhizobiaceae* family and lied next to each other in a single branch of a phylogenetic tree of the *Rhizobiaceae* family plotted with the ASVs as tip labels. We also performed an ANCOM test to find the significant different ASVs in the two amendments. Results were pretty similar to that of the Wilcox test. The ASVs that were significantly more abundant in ‘EEC-cross link’ amendment include ASV65, ASV69, ASV70, ASV72, ASV74, ASV80, ASV81, ASV83 and ASV85 which belong to the *Rhizobiaceae* family and ASV55 and ASV58 from the *Lactobacillaceae* family (Figure 31).

Same analyses were also performed for the negative cells to confirm if the interaction with these ASVs is specific to EECs. No significant ASV was found by the Wilcox test and the ASVs that were found to be significantly different by the ANCOM test (Figure 33) were completely different from the significant ASVs in the EEC cell population. Plotting the significant ASVs from the *Lactobacillaceae* family in EECs and negative cells on the phylogenetic tree (Figure 34) shows clear separation of the ASVs lying in two distinct branches. These results are completely novel and, to the best of our knowledge, have never been reported before.

## 6. Conclusion

This study suggests that altering the gut microbiota by using a single bacterial strain can modulate some of the behavioral phenotypes observed in rodents, including in autism mice model. While the underlying mechanism by which the gut microbiota sends signals to the brain remains to be explored, this study showed for the first time in rodents that specific taxa of the gut microbiota could directly interact with gut sensory cells. ASVs belonging to specific and homogeneous clades of the *Rhizobiaceae* and *Lactobacillaceae* families cross-linked with EECs. The recapitulation of connection between EECs and vagal neurons further suggests the involvement of the vagal afferent pathway as one of the mechanisms involved in gut microbiota-brain axis. Future work involving electrophysiological recordings of the EEC- neuron connection as well as transcriptomics to determine the production of synaptic proteins would confirm the synapse formation between EECs and vagus nerve. Since 16S rRNA sequencing has its limitations, we need to confirm our results with metagenomic sequencing and single cell sequencing to assess general cell response. Also, we need to explore the unexpected association of EECs with the *Rhizobiaceae* family as it has never been characterized before and confirm that it's not an artefact. Furthermore, exploring if metabolites of the ASVs associated with EECs from the *Rhizobiaceae* and *Lactobacillaceae* families can provoke electrical activity in the EECs, would further our understanding of how EECs modulate the brain functioning.

## Bibliography

- Agergaard, C. N., Hoegh, S. V., Holt, H. M., & Justesen, U. S. (2016). Two Serious Cases of Infection with *Clostridium celatum* after 40 Years in Hiding? *Journal of Clinical Microbiology*, *54*(1), 236–238.
- Angelis, M. D., De Angelis, M., Piccolo, M., Vannini, L., Siragusa, S., De Giacomo, A., Serrazzanetti, D. I., Cristofori, F., Guerzoni, M. E., Gobetti, M., & Francavilla, R. (2013). Fecal Microbiota and Metabolome of Children with Autism and Pervasive Developmental Disorder Not Otherwise Specified. In *PLoS ONE* (Vol. 8, Issue 10, p. e76993). <https://doi.org/10.1371/journal.pone.0076993>
- Bilbo, S. D., Levkoff, L. H., Mahoney, J. H., Watkins, L. R., Rudy, J. W., & Maier, S. F. (2005). Neonatal infection induces memory impairments following an immune challenge in adulthood. *Behavioral Neuroscience*, *119*(1), 293–301.
- Bohórquez, D. V., Chandra, R., Samsa, L. A., Vigna, S. R., & Liddle, R. A. (2011). Characterization of basal pseudopod-like processes in ileal and colonic PYY cells. *Journal of Molecular Histology*, *42*(1), 3–13.
- Bohórquez, D. V., Samsa, L. A., Roholt, A., Medicetty, S., Chandra, R., & Liddle, R. A. (2014). An Enteroendocrine Cell – Enteric Glia Connection Revealed by 3D Electron Microscopy. In *PLoS ONE* (Vol. 9, Issue 2, p. e89881). <https://doi.org/10.1371/journal.pone.0089881>
- Bohórquez, D. V., Shahid, R. A., Erdmann, A., Kreger, A. M., Wang, Y., Calakos, N., Wang, F., & Liddle, R. A. (2015). Neuroepithelial circuit formed by innervation of sensory enteroendocrine cells. *The Journal of Clinical Investigation*, *125*(2), 782–786.
- Bolivar, V. J. (2009). Intrasession and intersession habituation in mice: from inbred strain variability to linkage analysis. *Neurobiology of Learning and Memory*, *92*(2), 206–214.
- Bothe, G. W. M., Bolivar, V. J., Vedder, M. J., & Geistfeld, J. G. (2004). Genetic and behavioral differences among five inbred mouse strains commonly used in the production of transgenic and knockout mice. *Genes, Brain, and Behavior*, *3*(3), 149–157.
- Breit, S., Kupferberg, A., Rogler, G., & Hasler, G. (2018). Vagus Nerve as Modulator of the Brain-Gut Axis in Psychiatric and Inflammatory Disorders. *Frontiers in Psychiatry / Frontiers Research Foundation*, *9*, 44.
- Carabotti, M., Scirocco, A., Maselli, M. A., & Severi, C. (2015). The gut-brain axis: interactions between enteric microbiota, central and enteric nervous systems. *Annales de Gastroenterologie et D'hepatologie*, *28*(2), 203–209.
- Chandra, R., Samsa, L. A., Vigna, S. R., & Liddle, R. A. (2010). Pseudopod-like basal cell processes in intestinal cholecystokinin cells. *Cell and Tissue Research*, *341*(2), 289–297.

- Cryan, J. F., & Dinan, T. G. (2012). Mind-altering microorganisms: the impact of the gut microbiota on brain and behaviour. *Nature Reviews. Neuroscience*, *13*(10), 701–712.
- Das, M., & Fox, C. F. (1979). Chemical Cross-Linking in Biology. In *Annual Review of Biophysics and Bioengineering* (Vol. 8, Issue 1, pp. 165–193).  
<https://doi.org/10.1146/annurev.bb.08.060179.001121>
- David, M. M., Tataru, C., Daniels, J., Schwartz, J., Keating, J., Hampton-Marcell, J., Gottel, N., Gilbert, J. A., & Wall, D. P. (n.d.). *Crowdsourced study of children with autism and their typically developing siblings identifies differences in taxonomic and predicted function for stool-associated microbes using exact sequence variant analysis*.  
<https://doi.org/10.1101/319236>
- Diaz Heijtz, R., Wang, S., Anuar, F., Qian, Y., Björkholm, B., Samuelsson, A., Hibberd, M. L., Forssberg, H., & Pettersson, S. (2011). Normal gut microbiota modulates brain development and behavior. *Proceedings of the National Academy of Sciences of the United States of America*, *108*(7), 3047–3052.
- Engineer, C. T., Hays, S. A., & Kilgard, M. P. (2017). Vagus nerve stimulation as a potential adjuvant to behavioral therapy for autism and other neurodevelopmental disorders. *Journal of Neurodevelopmental Disorders*, *9*, 20.
- Feher, J. (2017). Intestinal and Colonic Chemoreception and Motility. In *Quantitative Human Physiology* (pp. 796–809). <https://doi.org/10.1016/b978-0-12-800883-6.00079-3>
- Finegold, S. M., Molitoris, D., Song, Y., Liu, C., Vaisanen, M.-L., Bolte, E., McTeague, M., Sandler, R., Wexler, H., Marlowe, E. M., Collins, M. D., Lawson, P. A., Summanen, P., Baysallar, M., Tomzynski, T. J., Read, E., Johnson, E., Rolfe, R., Nasir, P., ... Kaul, A. (2002). Gastrointestinal microflora studies in late-onset autism. *Clinical Infectious Diseases: An Official Publication of the Infectious Diseases Society of America*, *35*(Suppl 1), S6–S16.
- Goehler, L. E., Park, S. M., Opitz, N., Lyte, M., & Gaykema, R. P. A. (2008). *Campylobacter jejuni* infection increases anxiety-like behavior in the holeboard: possible anatomical substrates for viscerosensory modulation of exploratory behavior. *Brain, Behavior, and Immunity*, *22*(3), 354–366.
- Gribble, F. M., & Reimann, F. (2016). Enteroendocrine Cells: Chemosensors in the Intestinal Epithelium. *Annual Review of Physiology*, *78*, 277–299.
- Gunawardene, A. R., Corfe, B. M., & Staton, C. A. (2011). Classification and functions of enteroendocrine cells of the lower gastrointestinal tract. *International Journal of Experimental Pathology*, *92*(4), 219–231.
- Guo, P., Zhang, K., Ma, X., & He, P. (2020). Clostridium species as probiotics: potentials and challenges. In *Journal of Animal Science and Biotechnology* (Vol. 11, Issue 1).  
<https://doi.org/10.1186/s40104-019-0402-1>

- Hauschild, A. H. W., & Holdeman, L. V. (1974). *Clostridium celatum* sp. nov., isolated from normal human feces. *International Journal of Systematic and Evolutionary Microbiology*, 24(4), 478–481.
- Hefner, K., & Holmes, A. (2007). Ontogeny of fear-, anxiety- and depression-related behavior across adolescence in C57BL/6J mice. *Behavioural Brain Research*, 176(2), 210–215.
- Hsiao, E. Y. (2014). Gastrointestinal Issues in Autism Spectrum Disorder. In *Harvard Review of Psychiatry* (Vol. 22, Issue 2, pp. 104–111). <https://doi.org/10.1097/hrp.0000000000000029>
- Hsiao, E. Y., McBride, S. W., Hsien, S., Sharon, G., Hyde, E. R., McCue, T., Codelli, J. A., Chow, J., Reisman, S. E., Petrosino, J. F., Patterson, P. H., & Mazmanian, S. K. (2013). Microbiota modulate behavioral and physiological abnormalities associated with neurodevelopmental disorders. *Cell*, 155(7), 1451–1463.
- Hsiao, E. Y., & Patterson, P. H. (2011). Activation of the maternal immune system induces endocrine changes in the placenta via IL-6. *Brain, Behavior, and Immunity*, 25(4), 604–615.
- Kaelberer, M. M., Buchanan, K. L., Klein, M. E., Barth, B. B., Montoya, M. M., Shen, X., & Bohórquez, D. V. (2018). A gut-brain neural circuit for nutrient sensory transduction. *Science*, 361(6408). <https://doi.org/10.1126/science.aat5236>
- Kaidanovich-Beilin, O., Lipina, T., Vukobradovic, I., Roder, J., & Woodgett, J. R. (2011). Assessment of social interaction behaviors. *Journal of Visualized Experiments: JoVE*, 48. <https://doi.org/10.3791/2473>
- Kang, D.-W., Adams, J. B., Coleman, D. M., Pollard, E. L., Maldonado, J., McDonough-Means, S., Caporaso, J. G., & Krajmalnik-Brown, R. (2019). Long-term benefit of Microbiota Transfer Therapy on autism symptoms and gut microbiota. *Scientific Reports*, 9(1), 5821.
- Kang, D.-W., Adams, J. B., Gregory, A. C., Borody, T., Chittick, L., Fasano, A., Khoruts, A., Geis, E., Maldonado, J., McDonough-Means, S., Pollard, E. L., Roux, S., Sadowsky, M. J., Lipson, K. S., Sullivan, M. B., Caporaso, J. G., & Krajmalnik-Brown, R. (2017). Microbiota Transfer Therapy alters gut ecosystem and improves gastrointestinal and autism symptoms: an open-label study. *Microbiome*, 5(1), 10.
- Larsson, L., Goltermann, N., de Magistris, L., Rehfeld, J., & Schwartz, T. (1979). Somatostatin cell processes as pathways for paracrine secretion. In *Science* (Vol. 205, Issue 4413, pp. 1393–1395). <https://doi.org/10.1126/science.382360>
- Latorre, R., Sternini, C., De Giorgio, R., & Greenwood-Van Meerveld, B. (2016). Enteroendocrine cells: a review of their role in brain-gut communication. *Neurogastroenterology and Motility: The Official Journal of the European Gastrointestinal Motility Society*, 28(5), 620–630.
- Liddle, R. A. (2019). Neuropods. In *Cellular and Molecular Gastroenterology and Hepatology* (Vol. 7, Issue 4, pp. 739–747). <https://doi.org/10.1016/j.jcmgh.2019.01.006>

- Lopetuso, L. R., Scaldaferri, F., Petito, V., & Gasbarrini, A. (2013). Commensal Clostridia: leading players in the maintenance of gut homeostasis. *Gut Pathogens*, 5(1), 23.
- Lo, S.-C., Scearce-Levie, K., & Sheng, M. (2016). Characterization of social behaviors in caspase-3 deficient mice. *Scientific Reports*, 6, 18335.
- Lundberg, J. M., Tatemoto, K., Terenius, L., Hellström, P. M., Mutt, V., Hökfelt, T., & Hamberger, B. (1982). Localization of peptide YY (PYY) in gastrointestinal endocrine cells and effects on intestinal blood flow and motility. *Proceedings of the National Academy of Sciences of the United States of America*, 79(14), 4471–4475.
- Malkova, N. V., Yu, C. Z., Hsiao, E. Y., Moore, M. J., & Patterson, P. H. (2012). Maternal immune activation yields offspring displaying mouse versions of the three core symptoms of autism. *Brain, Behavior, and Immunity*, 26(4), 607–616.
- Martin, C. R., Osadchiy, V., Kalani, A., & Mayer, E. A. (2018). The Brain-Gut-Microbiome Axis. *Cellular and Molecular Gastroenterology and Hepatology*, 6(2), 133–148.
- May, C. L., & Kaestner, K. H. (2010). Gut endocrine cell development. In *Molecular and Cellular Endocrinology* (Vol. 323, Issue 1, pp. 70–75). <https://doi.org/10.1016/j.mce.2009.12.009>
- McDonald, D., Hyde, E., Debelius, J. W., Morton, J. T., Gonzalez, A., Ackermann, G., Aksenov, A. A., Behsaz, B., Brennan, C., Chen, Y., Goldasich, L. D., Dorrestein, P. C., Dunn, R. R., Fahimipour, A. K., Gaffney, J., Gilbert, J. A., Gogul, G., Green, J. L., Hugenholtz, P., ... Knight, R. (2018). American Gut: an Open Platform for Citizen Science Microbiome Research. *mSystems*, 3(3). <https://doi.org/10.1128/mSystems.00031-18>
- Messaoudi, M., Lalonde, R., Violle, N., Javelot, H., Desor, D., Nejdi, A., Bisson, J.-F., Rougeot, C., Pichelin, M., Cazaubiel, M., & Cazaubiel, J.-M. (2011). Assessment of psychotropic-like properties of a probiotic formulation (*Lactobacillus helveticus*R0052 and *Bifidobacterium longum*R0175) in rats and human subjects. In *British Journal of Nutrition* (Vol. 105, Issue 5, pp. 755–764). <https://doi.org/10.1017/s0007114510004319>
- Ming, X., Julu, P. O. O., Brimacombe, M., Connor, S., & Daniels, M. L. (2005). Reduced cardiac parasympathetic activity in children with autism. *Brain & Development*, 27(7), 509–516.
- Mohajeri, M. H., Hasan Mohajeri, M., La Fata, G., Steinert, R. E., & Weber, P. (2018). Relationship between the gut microbiome and brain function. In *Nutrition Reviews* (Vol. 76, Issue 7, pp. 481–496). <https://doi.org/10.1093/nutrit/nuy009>
- Moran, G. W., Leslie, F. C., Levison, S. E., Worthington, J., & McLaughlin, J. T. (2008). Enteroendocrine cells: neglected players in gastrointestinal disorders? *Therapeutic Advances in Gastroenterology*, 1(1), 51–60.
- Nagatake, T., Fujita, H., Minato, N., & Hamazaki, Y. (2014). Enteroendocrine cells are specifically marked by cell surface expression of claudin-4 in mouse small intestine. *PLoS*

*One*, 9(6), e90638.

- Parker, A., Fonseca, S., & Carding, S. R. (2020). Gut microbes and metabolites as modulators of blood-brain barrier integrity and brain health. *Gut Microbes*, 11(2), 135–157.
- Porges, S. W. (1995). Cardiac vagal tone: A physiological index of stress. In *Neuroscience & Biobehavioral Reviews* (Vol. 19, Issue 2, pp. 225–233).  
[https://doi.org/10.1016/0149-7634\(94\)00066-a](https://doi.org/10.1016/0149-7634(94)00066-a)
- Rehfeld, J. F. (1998). The New Biology of Gastrointestinal Hormones. In *Physiological Reviews* (Vol. 78, Issue 4, pp. 1087–1108). <https://doi.org/10.1152/physrev.1998.78.4.1087>
- Salvo-Romero, E., Stokes, P., & Gareau, M. G. (2020). Microbiota-immune interactions: from gut to brain. In *LymphoSign Journal* (Vol. 7, Issue 1, pp. 1–23).  
<https://doi.org/10.14785/lymphosign-2019-0018>
- Sternini, C., Anselmi, L., & Rozengurt, E. (2008). Enteroendocrine cells: a site of “taste” in gastrointestinal chemosensing. *Current Opinion in Endocrinology, Diabetes, and Obesity*, 15(1), 73–78.
- Sulfo-SBED Biotin Label Transfer Reagent*. (n.d.). Retrieved February 7, 2021, from <https://www.thermofisher.com/order/catalog/product/33033#/33033>
- Voreades, N., Kozil, A., & Weir, T. L. (2014). Diet and the development of the human intestinal microbiome. *Frontiers in Microbiology*, 5, 494.
- Weimer, B. C., Chen, P., Desai, P. T., Chen, D., & Shah, J. (2018). Whole Cell Cross-Linking to Discover Host-Microbe Protein Cognate Receptor/Ligand Pairs. *Frontiers in Microbiology*, 9, 1585.
- Worthington, J. J., Reimann, F., & Gribble, F. M. (2018). Enteroendocrine cells-sensory sentinels of the intestinal environment and orchestrators of mucosal immunity. *Mucosal Immunology*, 11(1), 3–20.
- Ye, L., Bae, M., Cassilly, C. D., Jabba, S. V., Thorpe, D. W., Martin, A. M., Lu, H.-Y., Wang, J., Thompson, J. D., Lickwar, C. R., Poss, K. D., Keating, D. J., Jordt, S.-E., Clardy, J., Liddle, R. A., & Rawls, J. F. (2020). Enteroendocrine cells sense bacterial tryptophan catabolites to activate enteric and vagal neuronal pathways. *Cell Host & Microbe*.  
<https://doi.org/10.1016/j.chom.2020.11.011>